

# CASE FILE COPY

N 68 33 516

**NASA TECHNICAL  
MEMORANDUM**

NASA TM X-52478

NASA TM X-52478

## STATISTICAL MECHANICAL THEORIES OF TRANSPORT PROPERTIES

by Richard S. Brokaw  
Lewis Research Center  
Cleveland, Ohio

TECHNICAL PAPER proposed for presentation at  
International Conference on the Properties of Steam  
Tokyo, Japan, September 9-13, 1968

NATIONAL AERONAUTICS AND SPACE ADMINISTRATION · WASHINGTON, D.C. · 1968

**STATISTICAL MECHANICAL THEORIES OF TRANSPORT PROPERTIES**

**by Richard S. Brokaw**

**Lewis Research Center  
Cleveland, Ohio**

**TECHNICAL PAPER proposed for presentation at  
International Conference on the Properties of Steam  
Tokyo, Japan, September 9-13, 1968**

**NATIONAL AERONAUTICS AND SPACE ADMINISTRATION**

# STATISTICAL MECHANICAL THEORIES OF TRANSPORT PROPERTIES

by Richard S. Brokaw

Lewis Research Center  
National Aeronautics and Space Administration  
Cleveland, Ohio

## INTRODUCTION

A detailed exposition of statistical mechanical theories of transport properties could easily fill a volume of many hundreds of pages. Such a treatise would involve difficult and sophisticated mathematics. And the presentation of this material could easily require one hundred hour-long lectures, a year-long course at the university graduate school level.

Fortunately our interests here are more modest. This conference is concerned with the properties of steam; we are interested in theories of transport properties insofar as theory can aid in selecting properties of water and steam. Consequently I will dwell principally on results rather than theoretical developments per se; results which have some bearing on the properties of steam.

The theories will be considered in turn as they relate to the following regimes:

1. The dilute gas
2. The dissociating gas (in the case of steam, temperatures in excess of 1700°C at atmospheric pressure)
3. The moderately dense gas
4. The gas in the critical region
5. The liquid state.

In all regimes save the last - the liquid state - theory may be of some help in selecting, correlating or predicting transport properties of steam.

### THE DILUTE GAS

Our discussion of the dilute gas will consider, first of all, the theory for monatomic gases, and then indicate what modifications are available to treat polyatomic gases.

#### Monatomic Gases

For dilute monatomic gases we have a very complete theory due to Chapman and Enskog. Their rigorous development is based on knowledge of the distribution function  $f_i(\underline{r}, \underline{V}_i, t)$ . This function represents the number of molecules of species  $i$  which lie in a unit volume about the point  $\underline{r}$  and have velocities within a unit range about  $\underline{V}_i$  at time  $t$ . If the gas is at equilibrium - that is, there are no gradients of composition, velocity, or temperature - then  $f_i(\underline{r}, \underline{V}_i, t)$  reduces to the Maxwellian distribution  $f_i^0 = n_i (m_i/2\pi kT)^{3/2} \exp(-m_i V_i^2/2kT)$ . When the system is not at equilibrium the distribution function satisfies the Boltzmann integro-differential equation.

We are interested in the properties of gases which are only slightly different from equilibrium, since it is only under these conditions that the fluxes are linear in the gradients so that the usual definitions of the transport coefficients apply. In this event the distribution function is nearly Maxwellian, and the Boltzmann equation can be solved by a perturbation

method due to Chapman and Enskog. The solutions are then used to obtain expressions for the fluxes and the transport coefficients. The method is set forth in great detail in the treatises of Chapman and Cowling (1) and Hirschfelder, Curtiss, and Bird (2).

The theory of Chapman and Enskog has the following restrictions: only binary collisions are considered, so that the results do not apply at densities where three-body collisions become important; all collisions are elastic; and pairs of molecules interact according to a single central force law so that the force depends only on the distance of separation between the molecules. Thus the Chapman-Enskog theory applies strictly only at moderate pressures and only to the noble gases.

The Chapman-Enskog theory yields the following expressions for the transport properties of dilute monatomic gases (3):

Viscosity

$$\eta = \frac{5}{16} \left( \frac{\sqrt{\pi m k T}}{\pi \sigma^2 \Omega^{(2,2)*}} \right) \quad (1)$$

Thermal conductivity

$$\lambda = \frac{25}{32} \left( \frac{\sqrt{\pi m k T}}{\pi \sigma^2 \Omega^{(2,2)*}} \right) \left( \frac{c_v}{m} \right) \quad (2)$$

Self-diffusion coefficient

$$D = \frac{3}{8} \left( \frac{\sqrt{\pi m k T}}{\pi \sigma^2 \Omega^{(1,1)*}} \right) \left( \frac{1}{\rho} \right) \quad (3)$$

These formulas involve quantities such as the atomic mass  $m$ , the Boltzmann constant  $k$ , the temperature  $T$ , the heat capacity  $c_v (= \frac{3}{2} k)$ , and the density

$\rho$ . Note that the viscosity and thermal conductivity are independent of density, or pressure, whereas the self-diffusion coefficient is inversely proportional to the density.

Equations (1)-(3) also involve cross sections, or more properly, collision integrals  $\sigma^2 \Omega^{(2,2)}$  and  $\sigma^2 \Omega^{(1,1)}$ , and to compute these the intermolecular force law must be known.

For a spherically symmetric potential, which may be written in a dimensionless form as

$$\frac{\phi(r)}{\epsilon} \equiv \phi^* = f(r/\sigma) = f(r^*) \quad (4)$$

the collision integrals are obtained by a triple integration. (Here  $\epsilon$  is an energy and  $\sigma$  is a distance characteristic of the potential.) First it is necessary to compute the angle of deflection:

$$\chi(g^*, b^*) = \pi - 2b^* \int_{r_m^*}^{\infty} \frac{dr^*/r^{*2}}{\sqrt{1 - (b^{*2}/r^{*2}) - (\phi^*/g^{*2})}} \quad (5)$$

where  $b^* = b/\sigma$  is the reduced impact parameter. (The impact parameter  $b$  is the distance of closest approach in the absence of the potential  $\phi$ .)

Further,  $r_m^* = r_m/\sigma$ , where  $r_m$  is the distance of closest approach in the presence of the potential, and  $g^{*2} = \frac{1}{4} mg^2/\epsilon$  is the reduced relative kinetic energy ( $g$  is the initial relative speed of the colliding molecules).

Once the angle of deflection has been obtained as a function of  $g^*$  and  $b^*$ , a velocity-dependent cross section is computed:

$$Q^{(l)*}(g^*) = \frac{2}{1 - \frac{1}{2} \{ [1 + (-1)^l] / (1+Q) \}} \int_0^\infty (1 - \cos^l \chi) b^* db^* \quad (6)$$

Finally, the  $Q^{(l)}$  are averaged over all velocities, with an appropriate weighting factor:

$$\Omega^{(l,s)*}(T^*) = \frac{2}{(s+1)! T^{*s+2}} \int_0^\infty e^{-g^{*2}/T^*} g^{*2s+3} Q^{(l)*} dg^* \quad (7)$$

Thus the collision integrals  $\Omega^{(l,s)*}$  are a function of reduced temperature  $T^* \equiv kT/\epsilon$ .

Hence the problem of a priori prediction of transport coefficients has three layers: first, a kinetic theory layer, which relates the transport coefficients to the collision cross sections, via equations (1)-(3); second, a cross section layer, which relates the collision integrals to the intermolecular forces via equations (5)-(7); and finally the core problem of determining the intermolecular forces (equation (4)).

In principle, the intermolecular forces can be calculated from quantum mechanics, given only fundamental constants such as the electronic charge and mass and Planck's constant. In practice it is not yet possible to carry out such calculations with sufficient accuracy except for simple systems, such as two hydrogen atoms or perhaps two helium atoms (4). For more complicated systems severe approximations have to be introduced so that the results are not likely to be quantitatively accurate. It is to be hoped, however, that the calculations are qualitatively correct and thus

indicate the general form of the intermolecular potential.

Since the intermolecular force law is not known a priori, the usual procedure is to let theory indicate the probable form of the force law, assume some analytic form for the potential which has the correct theoretical behavior, and use experimental data to evaluate the adjustable parameters in the analytic potential. Experimental information from transport properties, second virial coefficients, and molecular beam scattering can be used in this fashion (5). The collision integrals have now been calculated for a number of analytic potentials; available tabulations of collision integrals have been summarized recently by Mason (6).

Despite the fact that the theory for dilute monatomic gases seems well established there have been experimental anomalies which have only recently been resolved. This is illustrated in figure 1, where viscosity data for argon are present. (The quotient of viscosity and temperature is plotted since this function is less temperature dependent than the viscosity itself so that discrepancies are more clearly revealed.) The open symbols are experimental data from the older literature due to Trautz and Binkele (7) (triangles), Trautz and Zink (8) (squares), and Vasilesco (9) (circles). These data are not in accord with viscosities calculated by Amdur and Ross (10) from a potential energy function deduced from high energy atomic beam scattering experiments (11). Very recent experimental data, shown as filled symbols, indicate that the older viscosities are considerably in error at the higher temperatures. These new results include the precise data of DiPippo and Kestin (12) in the range 25-300°C and



unpublished Los Alamos data due to Guevara, McInteer, and Wageman (13) in the range 1100-2100°K. The solid line in figure 1 is a fit of a modified Buckingham (exp-6) potential to the data of references (12) and (13) due to Hanley and Childs (14); this fit reproduces the experimental data of DiPippo and Kestin (12) within 0.4% and Guevara, McInteer, and Wageman (13) within 1%.

Hanley and Childs (14) also point out that heat conductivities calculated from this same fit are in reasonable agreement with experiment, whereas values calculated from a fit to the older viscosity data (7), (8), (9), appear systematically low at the higher temperatures. To make the same point in a slightly different fashion, equations (1) and (2) can be combined to give a relation between heat conductivity and viscosity for monatomic gases<sup>\*</sup>:

$$\lambda = \frac{5}{2} \frac{C_v}{m} \eta = \frac{15}{4} \frac{R}{M} \eta \quad (8)$$

Thus equation (8) permits us to calculate heat conductivities from viscosities. It is found that heat conductivities calculated from the newer viscosity data of references (12) and (13) are in good agreement with

---

\* Equations (1) and (2) are the lowest Chapman-Enskog approximations; if higher approximations are included the numerical factors in equation (8) are increased slightly. In the case of argon, with the exp-6 potential of Hanley and Childs, this increase amounts to 0.06% at room temperature and increases to 0.4% at 2000°K. (Calculated from Table VII C, pp. 1173 and 1174 of Ref. 2.)

experimental conductivities whereas values calculated from the older literature (refs. 7-9) are somewhat low at the higher temperatures.

The reconciliation of these experimental anomalies in the transport properties of argon can be of help in selecting transport properties of steam. Consider, for example, the experimental viscosities of steam measured by Bonilla, Wang and Weiner (15). This work covered a wide temperature range, approximately 250-1450°C, but the values lie from 2.5 to 4 percent below the more recent and presumably more reliable measurements of Shifrin (16) and Kestin and Richardson (17). Consequently the data of Bonilla, Wang and Weiner were not used in setting up the skeleton tables for viscosity established by the Sixth International Conference on the Properties of Steam (18).

The data of Bonilla et. al. are not absolute; rather the apparatus was calibrated with nitrogen assuming the nitrogen viscosities of Vasilescu (9). Fortunately Bonilla and coworkers (15) also measured the viscosity of argon in the same temperature range; so we can use their argon data to correct their steam data on the basis of the (exp-6) potential fit to recent argon viscosities (12), (13). Thus

$$\eta_{H_2O, \text{corrected}} = \eta_{H_2O, \text{ref. 15}} \frac{\eta_{Ar, \text{exp-6}}}{\eta_{Ar, \text{ref 15}}} \quad (9)$$

The corrected viscosities shown in figure 2 are in good agreement with the results of Shifrin (16), Latto (19) and the skeleton tables to 700°C. At higher temperatures the corrected viscosities lie above the data of Shifrin

and Latto; the discrepancy amounts to 3.4% at 1100°C. Thus the corrected viscosities of Bonilla et. al. are now in substantial agreement with the more recent literature.

Because we have a rigorous theory for monatomic gases we can compute heat conductivities from experimental viscosities (equation (8)); and because it is usually easier to measure viscosity with good precision and accuracy such computed heat conductivities for argon are probably better than experimental values. These computed conductivities can help in selecting heat conductivities for steam. For example, Geier and Schäfer (20) have measured heat conductivities of steam, nitrogen, and a number of other gases in the range 100-1000°C. Their steam data at the higher temperatures lie almost ten percent below the smoothed results of Vargaftik and Zimina (21), which are the basis of low pressure skeleton tables for the thermal conductivity of steam (18). Unfortunately Geier and Schäfer did not measure heat conductivities for argon, so it is not possible to correct their conductivities directly. However, Vargaftik and Zimina (22) have measured heat conductivities of argon in the range 0-1000°C and their results are in good agreement with predictions from the (exp-6) potential fit to the recent viscosity data (14). Vargaftik and Zimina (23) have also measured heat conductivities of nitrogen, so it is possible to correct the Geier and Schäfer data indirectly as follows:

$$\lambda_{H_2O, corrected} = \lambda_{H_2O, GS} \frac{\lambda_{N_2, VZ}}{\lambda_{N_2, GS}} \frac{\lambda_{Ar, exp-6}}{\lambda_{Ar, VZ}} \quad (10)$$

in this equation subscripts GS refer to the Geier and Schäfer data (20) while subscripts VZ refer to the Vargaftik and Zimina results (22) and (23).

Heat conductivities corrected by means of equation (10) are shown as half-filled circles in figure 3. Also shown are the uncorrected values (unfilled circles), and the high temperature values of Vargaftik and Zimina (21) (squares). At high temperatures this correction halves the discrepancy between the Geier and Schäfer (20) and Vargaftik and Zimina (21) results.

Vargaftik and Zimina (21) point out that Geier and Schäfer (20) did not apply a temperature jump correction to their steam data. To calculate this correction one needs to know the geometry and dimensions of the apparatus, the gas pressure, and the accommodation coefficients of the surfaces. An elementary theory of this phenomenon is given by Kennard (24). The correction takes the form

$$\lambda_{\text{corrected}} = \lambda_{\text{measured}} (1 + \beta). \quad (11)$$

For a concentric cylinder geometry,

$$\beta = \frac{2-a}{a} \frac{(2\pi MRT)^{1/2}}{r_1 \ln(r_2/r_1)} \frac{\lambda}{(2C_p - R)P} \quad (12)$$

where  $a$  is the accommodation coefficient of the inner cylinder,  $r_1$  and  $r_2$  are the radii of the inner and outer cylinders,  $C_p$  is the molar heat capacity at constant pressure,  $R$  is the molar gas constant,  $P$  is the pressure, and  $M$  is the molecular weight. We can calculate lower limit values of  $\beta$  for Geier and Schäfer's data by assuming  $a = 1$  and  $P \sim 20$  mm Hg, the vapor

pressure of water at room temperature<sup>\*</sup>.

Heat conductivities of steam corrected for temperature jump using equations (11) and (12) are shown as filled circles in figure 3. The corrected data lie somewhat above the skeleton tables and the results of Vargaftik and Zamina (21) (the average deviation is +2.6%).

Thus we see that the fact that we have a rigorous theory for the transport properties of monatomic gases can be helpful in selecting and evaluating data on polyatomic gases including steam. Experimentalists should be urged to include measurements on the noble gases, especially helium and argon. In this way their data can be reevaluated in the future when the intermolecular potentials for the noble gases are known with greater accuracy. It seems most likely that we will first get such information for the noble gases, both from experiment and more sophisticated quantum mechanical calculations. It will be a long time before detailed information is available on polyatomic gases (with the possible exception of  $H_2$ ).

### Polyatomic Gases

When we come to consider polyatomic gases we recall that the Chapman-Enskog theory assumes molecules interact according to a central force law and that all collisions are elastic. If we wish to extend or approximate

---

\* Geier and Schäfer (20) give their wire diameter as  $0.1 \text{ mm} = 2r_1$  but do not report the diameter of the outer cylinder. A later paper describing a similar apparatus gives  $2r_2 = 16 \text{ mm}$  (25). The exact value is not crucial, since  $r_2$  appears only logarithmically in equation (12).

the theory for polyatomic gases we must consider the effects of orientation-dependent forces and inelastic collisions.

Orientation-dependent forces introduce two complications. First, they provide a mechanism for interchange of rotational and translational energy; in other words they introduce inelastic collisions. Secondly, the orientation-dependent forces complicate the molecular collision trajectories so that the numerical integrations necessary for obtaining the collision integrals are almost impossibly difficult.

Monchick and Mason (26), in a paper dealing with transport properties of polar gases, circumvented these two complications by introducing two assumptions which they justified on physical grounds.

First they assumed that the inelastic collisions, even though they occur frequently, have little effect on the trajectories. They argue that most inelastic collisions involve the transfer of only a few quanta of rotational energy; for most molecules this is small compared to the translational energy which is of the order of  $kT$ . Hence they assume that inelastic collisions, on the average, have little effect on the trajectories.

Their second assumption concerns the effect of orientation-dependent forces on the angle of deflection  $\chi$  (equation (5)). They argue that although the orientation-dependent forces act along the whole trajectory, the angle of deflection is determined primarily by the interaction in the vicinity of the distance of closest approach. Over a small range near the distance of closest approach the relative orientation does not change much, so that in each collision  $\chi$  is determined largely by only one relative

orientation.

These two assumptions change the problem of orientation-dependent forces from difficult collision dynamics to easier kinetic theory. The kinetic theory problem corresponds to a gas in which collisions follow not one intermolecular force law, but any one of a very large number of force laws, one for each relative orientation. This problem has been solved (27); the expressions for the transport coefficients are the same as for a single interaction potential, but the cross sections or collision integrals are averages over all possible force laws.

The most realistic intermolecular potential which has been considered for the transport properties of polar gases is the Stockmayer potential

$$\phi(r) = 4\epsilon \left[ \left( \frac{\sigma}{r} \right)^{12} - \left( \frac{\sigma}{r} \right)^6 - g \delta \left( \frac{\sigma}{r} \right)^3 \right] \quad (13)$$

where

$$g = \frac{1}{2} \left[ 2 \cos \theta_a \cos \theta_b - \sin \theta_a \sin \theta_b \cos \psi \right] \quad (14)$$

and

$$\delta \equiv \frac{1}{2} \frac{\mu^2}{\epsilon \sigma^3} \quad (15)$$

Here  $\mu$  is the dipole moment,  $\theta_a$  and  $\theta_b$  are the angles of inclination of the dipole axes to the line joining the centers of the molecules, and  $\psi$  is the azimuthal angle between them. When there is no dipole moment

equation (13) reduces to the familiar Lennard-Jones (12-6) potential with an attractive well depth  $\epsilon$  and a zero energy collision diameter  $\sigma$ , which is a measure of the size of the molecule.

Equation (13) has: an inverse twelfth power repulsive force to crudely approximate the strong repulsive forces between molecules at small separations; an inverse sixth power attractive term, a reasonable representation of the long range attractive forces for nonpolar gases; and an angle-dependent inverse cube power term, which represents the interaction between point dipoles located at the centers of the molecules.

Monchick and Mason (26) have approximated collision integrals subject to the assumptions mentioned above; they approximate  $g$  (equation (14)) throughout a collision by a constant  $g_0$ , presumably the value of  $g$  at the distance of closest approach. This is equivalent to replacing equation (13) with a multitude of spherically symmetrical potentials corresponding to all values of  $g_0$  between -1 and +1. The collision integrals were then evaluated and averaged over all relative orientations.

This, then, is the most sophisticated theoretical model available for the properties of steam. Since the dipole moment of steam is well established (1.85 Debye (28)), there are two disposable parameters available,  $\sigma$  and  $\epsilon$ , for fitting viscosity data on steam.

Results of an attempt to fit the approximate Stockmayer potential collision integrals (26) to experimental viscosity data on steam are shown in figure 4, where the viscosity-temperature quotient is plotted as a function of temperature. The solid curve has been calculated for



$\sigma = 2.4934 \text{ \AA}$ ,  $\epsilon/k = 800^\circ\text{K}$ , and  $\delta = 1.0$ ; this is consistent with the experimental dipole moment of 1.85 Debye (one Debye =  $10^{-18}$  esu cm). The fit is rather poor; it is nearly 5% above the skeleton table at  $100^\circ\text{C}$  and 6% below at  $700^\circ\text{C}$ . Qualitatively, the experimental viscosities increase more rapidly with temperature up to about  $700^\circ\text{C}$ ; at higher temperatures the reverse is true and the experimental viscosities increase less rapidly than theory based on the approximate Stockmayer collision integrals.

Somewhat better agreement can be obtained by treating  $\delta$  as another disposable parameter; such a fit is shown as the dashed curve in figure 4, calculated for  $\sigma = 2.525 \text{ \AA}$ ,  $\epsilon/k = 370^\circ\text{K}$ , and  $\delta = 2.5$  (the largest value for which the collision integrals have been calculated (26)). This corresponds to an effective dipole moment of 2.028 Debye, nearly ten percent in excess of experiment. Although the fit to experiment is improved it is still not good (in contrast, for example, to the excellent fit of the exponential-6 potential to the argon data, shown in figure 1). Further, there is no theoretical justification for allowing  $\delta$ , (or the dipole moment) to be a disposable parameter.

We conclude that the approximate Stockmayer collision integrals cannot be fit to the viscosity data of steam. Thus they are nearly useless insofar as prediction of properties under other conditions is concerned; they cannot be used for interpolation, let alone extrapolation.

It is not easy to pinpoint the reasons for this failure. First of all, the Stockmayer potential is perhaps a rather poor approximation to the force law between water molecules; the charge distribution within the

molecule is probably not adequately represented by a point dipole. The next logical step would be to add a dipole-quadrupole term to the force law, as Rowlinson (30) has done to obtain improved agreement between theory and experiment for the second virial coefficients of steam. The collision integrals could then be approximated in the same way that the cross sections for the Stockmayer potential have been approximated (26).

On the other hand we do not know what errors may be introduced by Monchick and Mason's assumptions that inelastic collisions have little effect on trajectories and that the angle of deflection in a collision is determined by the relative orientation at the distance of closest approach. Perhaps these assumptions could be tested by some judicious computer studies of collision dynamics.

Let us turn now to the question of inelastic collisions. We may be able to neglect inelastic collisions in considering viscosity and diffusion coefficients, which depend on molecular momentum and mass; but we must expect larger errors if we neglect such collisions in considering the heat conductivity of polyatomic gases, since this property depends on the transport of both translational and internal energy.

It is convenient to discuss the thermal conductivity of a polyatomic gas in terms of its relationship to the viscosity through the dimensionless ratio

$$f \equiv \lambda M / \eta C_v \quad (16)$$

According to ultrasimplified kinetic theory,  $f = 1$ ; however, the rigorous

Chapman-Enskog theory for monatomic gases predicts that  $f$  should be very nearly  $5/2$  (see equation (8)). This is due to the fact that translational energy is a function of molecular velocity; the molecules possessing the most energy are the most rapid, have the longest mean free paths, and hence make an enhanced contribution to the heat transport.

For polyatomic gases,  $f$  is less than  $5/2$  and tends to be small when the molar heat capacity is large and originates mostly from the internal energy modes. Consequently Eucken (31) suggested that the transport of translation and internal energy be considered separately, and proposed

$$fC_v = f_{\text{trans}}C_{v, \text{trans}} + f_{\text{int}}C_{\text{int}} \quad (17)$$

( $C_{v, \text{trans}}$  and  $C_{\text{int}}$  are the translational and internal contributions to the total heat capacity  $C_v$ .) Eucken assumed  $f_{\text{trans}} = 5/2$ , by analogy with the monatomic gases. However, because there is expected to be little correlation between molecular velocity and internal energy, Eucken assumed  $f_{\text{int}} = 1$ , the result of the ultra-simple theory.

Ubbelohde (32) pointed out that molecules with excited internal energy states may be regarded as different chemical species and that the flow of internal energy can be considered as energy transport due to diffusion of the excited states. This concept leads to the result

$f_{\text{int}} = \rho D_{\text{int}} / \eta$ , so that

$$f_{\text{ME}} = \frac{15}{4} R + \frac{\rho D_{\text{int}}}{\eta} C_{\text{int}}, \quad (18)$$

which is known as the modified Eucken approximation. Here  $D_{\text{int}}$  is a

diffusion coefficient for internal energy; if  $D_{int}$  is taken to be the self-diffusion coefficient then  $f_{int} \approx 1.3$ . To justify this modified Eucken approximation (equation(18)) it is tacitly assumed that inelastic collisions are rare. This is necessary in order that the translational velocity distribution function should not be unduly perturbed, so that the translational conductivity can be related to the viscosity as in the case of the noble gases. On the other hand, there must be enough inelastic collisions to maintain the internal energy states in equilibrium with the local temperature.

In order to account for inelastic collisions in a rigorous fashion it is necessary to reformulate the Boltzmann equation, and then carry out the solution by an extension of the Chapman-Enskog method which allows for inelastic processes.

Theories of this sort were first developed by Wang Chang, Uhlenbeck, and deBoer (33), (34), and by Taxman (35). Although these formally solve the kinetic theory problem, they cannot be used to predict transport coefficients because the task of calculating the cross sections or collision integrals involving inelastic collision appears hopelessly difficult.

However Mason and Monchick (36) have succeeded in developing explicit expressions relating the heat conductivity of a polyatomic gas to other gas properties, starting with the purely formal theories of refs. (33), (34). By systematically including terms involving inelastic collisions, they derived the modified Eucken expression (equation (18)) as a first

approximation and, as a second approximation, an expression dependent on the relaxation times for the various internal degrees of freedom. Their result may be written

$$f_{MM}C_v = \frac{15}{4} R + \frac{\rho D_{int}}{\eta} C_{int} - \frac{\frac{2}{\pi} \left( \frac{5}{2} - \frac{\rho D_{int}}{\eta} \right)^2 \sum \frac{C_k}{Z_k}}{1 + \frac{2}{\pi} \left( \frac{5}{3R} + \frac{\rho D_{int}}{\eta C_{int}} \right) \sum \frac{C_k}{Z_k}} \quad (19)$$

Here  $Z_k$  is the number of collisions for relaxation of the  $k$ th internal mode while  $C_k$  is the heat capacity associated with that mode. The collision number is related to the relaxation time  $\tau_k$ :

$$Z_k = \frac{\tau_k}{\tau_{coll}} = \frac{4}{\pi} \frac{P \tau_k}{\eta} \quad (20)$$

where  $\tau_{coll} = (\pi/4) (\eta/P)$  is the mean time between collisions.

The first two terms in equation (19) are simply the modified Eucken approximation while the third term is important only for modes involving small collision numbers. In small, rigid polyatomic molecules these are associated with rotational relaxation. For example, in the case of steam, for rotation  $Z_{rot} \sim 4$  whereas for vibration  $Z_{vib} \sim 70-80$  (37), (38). (In large flexible molecules vibrational relaxation times may also be small.)

In Mason and Monchick's expression (equation (19)) the difficult integrals of the formal theory are disguised in the  $Z_k$  and in  $D_{int}$ , the diffusion coefficient for internal energy. The theoretical expression for  $Z$  is complicated, as might be expected, and has only been evaluated for

very simplified and unrealistic models such as spherocylinders and rough and loaded spheres (39), (40). Fortunately the collision numbers can be obtained experimentally from acoustical studies or shock tube measurements.

The situation with respect to the diffusion coefficient for internal energy is less fortunate. Again it can be calculated only for simplified and unrealistic molecular models, but in this case there does not seem to be any experimental method independent of the heat conductivity itself. For lack of a better procedure,  $D_{int}$  is commonly assumed equal to the self diffusion coefficient for nonpolar gases.

However, the thermal conductivities of highly polar gases, including hydrogen fluoride, steam, and ammonia appear to be anomalously low in relation to their viscosities. Mason and Monchick (36) suggest that this effect is largely due to a resonant exchange of rotationed energy, presumed probably on grazing self-collisions of polar molecules. Hence, a grazing collision with exchange is equivalent to a head-on collision without exchange, insofar as the transport of the rotational quantum is concerned. Thus the diffusion coefficient for internal energy,  $D_{int}$ , is smaller than the self-diffusion coefficient,  $D$ , and is given by the expression

$$D_{int} = D/(1 + \Delta) \quad (21)$$

where  $\Delta$  is a correction term calculated from the theory of resonant collisions. Mason and Monchick (36) give expressions for  $\Delta$  for linear dipoles and also for several types of symmetric tops.

This theory has had success in rationalizing experimental data on a number of nonpolar gases (36), (41); in the case of polar gases it seems

to do a good job of describing the changes due to isotopic substitution of deuterium for hydrogen (42)-(44)\*. Consequently it may be worthwhile to see if the theory can successfully predict heat conductivities of steam from experimental viscosities. Inasmuch as  $Z_{vib}$  is 70-80 for steam we can neglect it and consider only rotational relaxation. Equation (19) is then rewritten to calculate conductivity,

$$\lambda_{H_2O} = \frac{\eta_R}{M} \left[ \frac{15}{4} + \frac{\rho_{D_{int}}}{\eta} \frac{c_{int}}{R} - \frac{\frac{3}{\pi^2_{rot}} \left( \frac{5}{2} - \frac{\rho_{D_{int}}}{\eta} \right)^2}{1 + \frac{2}{\pi^2_{rot}} \left( \frac{5}{2} + \frac{\rho_{D_{int}}}{\eta} \right)} \right]. \quad (22)$$

The dimensionless group  $\rho_{D_{int}}/\eta$  can be calculated from an equation obtained by combining equations (1), (3), and (21)

$$\frac{\rho_{D_{int}}}{\eta} = \frac{(6/5) \Omega^{(2,2)*} / \Omega^{(1,1)*}}{1 + \Delta}. \quad (23)$$

The ratio of collision integrals  $\Omega^{(2,2)*} / \Omega^{(1,1)*}$  is a slowly varying function of temperature whose exact value depends on the intermolecular force law. However, for most realistic potentials this ratio is close to 1.1, so we can use values based on the Stockmayer potential with some

---

\* References (36) and (41)-(44) actually used an approximation to equation (19) obtained by taking the denominator of the third term in equation (19) to be unity.

confidence. (For this potential the ratio varies between 1.074 at 100°C and 1.108 at 1000°C.)

As was already mentioned, Mason and Monchick (36) developed expressions for the resonant corrections,  $\Delta$ , for linear dipoles and symmetric tops. They suggest that slightly asymmetric tops can be treated in the following manner. If  $I_A$  is the moment of inertia about the dipole axis (in the case of water, the figure axis of the molecule) and  $I_B$ ,  $I_C$  are the other two moments, one uses the symmetric top formulas replacing  $I_B$  by  $(I_B I_C)^{1/2}$ . In point of fact, the water molecule is a highly asymmetric top ( $I_B$  and  $I_C$  differ by a factor of three). In the absence of any better procedure we will assume that water can be treated as a slightly asymmetric top and find that it must then be classed as a near-spherical top. For such molecules,

$$\Delta = \pi^{3/2} \langle a_4 \rangle \left( \frac{3}{16} \frac{\mu h}{kT} \right)^2 \frac{\Omega_{(2,2)}^{(2,2)*}}{\Omega_{(1,1)}^{(1,1)*}} \frac{\eta}{\sqrt{kT}} \frac{R/C_{int}}{I_A (I_B I_C)^{1/2}} \left[ \frac{5}{4} - \frac{(I_B I_C)^{1/2}}{4 I_A} \right]^{-7/2} \quad (24)$$

Here  $\langle a_4 \rangle$  is the mean value of a dimensionless quantity involving the rotational quantum numbers, taken to be 0.44 and  $h$  is Planck's constant.

Heat conductivities for steam calculated from equations (22)-(24) are compared with experiment in fig. 5. The calculations (carried out at 100°, 300°, 500°, 700° and 1000°C) are based on skeleton table viscosities to 700°C (18) and Latto's value at 1000°C (19). The collision number for rotational relaxation was taken to be four (37), (38).

Although the agreement between theory and experiment is good at 100°C,



predicted heat conductivities are uniformly about 13% too high at temperatures above 300°C. If Mason and Monchick's (36) expression for the heat conductivity is correct, the difficulty must lie in our inability to properly predict  $D_{int}$  rather than  $Z_{rot}$ , because even if it is assumed that both  $Z_{rot}$  and  $Z_{vib}$  are zero, the predicted conductivity at 1000°C is still 3-5% too large.

Thus the theory of Mason and Monchick (36) cannot at this time be used for predicting heat conductivities for steam, nor can the theory help us in selecting among discordant experimental data. This theory may become useful in the future if reliable experimental or theoretical methods are developed for determining the diffusion coefficient for internal energy  $D_{int}$  and also (to a lesser extent) high temperature relaxation times.

To summarize briefly regarding the dilute gas: the theory for monatomic gases is in good shape and can be helpful in selecting and correcting experimental viscosities and heat conductivities of steam; available theories for polyatomic gases do not correlate steam data at all well. Theoretical prediction of viscosity may become feasible when the intermolecular potential for steam is known in greater detail and the appropriate collision integrals are evaluated numerically. Theoretical prediction of heat conductivity may be possible when methods are developed for obtaining relaxation times and diffusion coefficients for internal energy.

## THE DISSOCIATING GAS

If the temperature is raised sufficiently, polyatomic molecules dissociate into simpler fragments. As an example, the equilibrium composition of steam at atmospheric pressure is shown as a function of temperature in figure 6 (45). At about  $2100^{\circ}$ - $2300^{\circ}$ K water starts to dissociate and the diatomic molecules  $H_2$ ,  $OH$ , and  $O_2$  appear. The concentrations of these species maximize at  $3400^{\circ}$ - $3500^{\circ}$ K where they comprise almost forty percent of the gas mixture; at higher temperatures they too dissociate. Hydrogen and oxygen atoms appear in the range  $2600^{\circ}$ - $2800^{\circ}$ K and increase; they account for more than ninety percent of the mixture at  $4500^{\circ}$ K.

The transport properties of a dissociating gas can be treated in terms of dilute gas theory; however two new features appear. First of all, we are dealing with a mixture of gases rather than a single chemical species. Secondly, the presence of mobile chemical equilibria can lead to a large increase in the thermal conductivity.

Theories for the transport properties of gas mixtures are about as well-developed as theory for pure gases. Thus the Chapman-Enskog method has been developed for the viscosity (46) and thermal conductivity (47) of multicomponent monatomic gas mixtures. Hirschfelder (48), (49) has derived an expression for the heat conductivity of polyatomic gas mixtures which is equivalent to the modified Eucken approximation for pure gases, while Monchick, Pereira, and Mason (50) have obtained an expression for polyatomic gas mixtures analogous to the Monchick-Mason theory (36) for pure gases.

These expressions for gas mixtures are algebraically much more complex than corresponding expressions for pure gases, but if a computer is available this is merely a matter of bookkeeping. In addition, the expressions involve cross sections characteristic of all pairwise interactions in the gas mixture. In a mixture of  $\nu$  components there are  $\nu(\nu+1)/2$  interactions, so a great deal of information about the various intermolecular force laws is required.

Svehla (45) has calculated the transport properties of steam in the range 600°-5000°K. The calculations are not based on any single intermolecular force law, but rather a variety of potentials more or less appropriate to the various interactions. Calculated viscosities are shown in figure 7; also shown are the skeleton table values and the highest temperature data of references (15) (corrected) and (19). Svehla used Stockmayer potential force constants for the H<sub>2</sub>O-H<sub>2</sub>O interaction which were fit to the uncorrected data of reference (15) and for that reason his computed viscosities lie below the experimental values. Note that above 3000°K the viscosity becomes pressure-dependent because the gas composition changes considerably with pressure. (At low pressures the viscosity of a pure gas is independent of pressure, see equation (1).)

Let us turn now, to the second and more dramatic phenomenon in dissociating gases. In dissociating gases heat transport may be much larger than in "frozen" (nonreacting) mixtures. Large amounts of heat can be carried as chemical enthalpy of molecules that diffuse because the gas composition varies with temperature. For example, in a gas that

absorbs heat by dissociating as the temperature is raised heat is transported when a molecule dissociates in the high-temperature region and the fragments diffuse toward the cooler region. In the low-temperature region the fragments recombine and release the heat absorbed at high temperature.

When the chemical reaction rates are very high, chemical equilibrium can be assumed to exist locally throughout a gas mixture. It is then possible, by differentiating the equilibrium relations, to relate the concentration gradients to the temperature gradient. In this event one can define an equilibrium thermal conductivity  $\lambda_e$  independent of apparatus geometry and scale:

$$\lambda_e = \lambda_f + \lambda_r \quad (25)$$

where  $\lambda_f$  is the conductivity in the absence of reaction (the "frozen" thermal conductivity) and  $\lambda_r$  is the augmentation due to the reactions.

A general expression for the thermal conductivity due to chemical reactions has been developed (51), (52) that is applicable to mixtures involving any number of reactants, inert diluents, and chemical equilibria, provided chemical equilibrium exists locally in the temperature gradient. For a simple dissociation of the type  $A \rightleftharpoons nB$  the thermal conductivity due to chemical reaction is

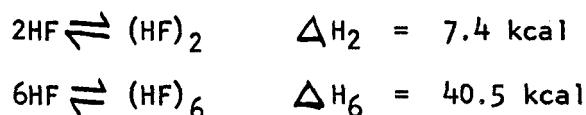
$$\lambda_r = \frac{D_{AB}P}{RT} \frac{\Delta H^2}{RT^2} \frac{x_A x_B}{(n x_A + x_B)^2} \quad (26)$$

Here  $D_{AB}$  is the binary diffusion coefficient between components A and B,  $\Delta H$  is the heat of reaction, and  $x_A$ ,  $x_B$  are the mole fractions of the components. Note that unless both species are present,  $\lambda_r$  is zero. Further-

more, since in a dissociating gas the composition varies with pressure, we expect the heat conductivity to vary with pressure also. This is in contrast to the behavior of nonreacting gases, for which the heat conductivity is independent of pressure.

Experimental (53) and theoretical (54) conductivities for the  $\text{N}_2\text{O}_4 \rightleftharpoons 2\text{NO}_2$  system at one atmosphere are shown in figure 8. The dashed curve indicates the frozen conductivity. Thus  $\lambda_f$  is the major contribution to the heat conductivity; at the maximum (where the mass fractions of  $\text{N}_2\text{O}_4$  and  $\text{NO}_2$  are equal) the conductivity is comparable to that of a light gas such as helium, and an order of magnitude greater than in the chemically frozen gas mixture.

The theoretical expression for a system involving two reactions has been tested (55) for the case of hydrogen fluoride vapor. At moderate pressures the PVT behavior of hydrogen fluoride can be described in terms of a monomer-hexamer equilibrium, while low pressure data suggest a dimer as well. Although the actual state of the vapor is uncertain, it appears that at low and moderate pressures the equilibria



serve to specify the system rather well.

Computed and experimental (56) thermal conductivities are compared in fig. 9. The solid line was computed assuming both dimer and hexamer equilibria, whereas the dashed line was computed considering only the hexamer equilibrium. Note the extreme pressure dependence of the thermal

conductivity. The maximum conductivity is more than three times that of hydrogen at the same temperature and some 33 times the frozen thermal conductivity expected in the absence of reaction. The inclusion of a dimer equilibrium markedly improves the agreement between theory and experiment in the low-pressure region.

The experimental studies on nitrogen tetroxide and hydrogen fluoride prove the validity of the theoretical expressions for thermal conductivity of reacting gases in chemical equilibrium. The theory has also been successfully applied to data for the  $\text{PCl}_5 \rightleftharpoons \text{PCl}_3 + \text{Cl}_2$  equilibrium.

Svehla (45) has calculated the thermal conductivity of equilibrium steam at temperatures from  $600^\circ$  to  $5000^\circ\text{K}$ . His results at 0.1 and 10 atmospheres are shown in figure 10; this system involves four simultaneous equilibria. The solid curves are the equilibrium conductivities; in the regions of the maxima they are an order of magnitude larger than the frozen conductivities (dashed curves).

Since Svehla's calculations of viscosity and heat conductivity use dilute gas theory which show deviations from experiment of ten percent or more at lower temperatures (figures 4 and 5) we may expect comparable or larger errors in the high temperature regime, perhaps on the order of twenty percent. These calculations may be useful nonetheless, as it is likely to be some time before experimental data of this accuracy are available for temperatures much in excess of  $2000^\circ\text{K}$ .

The theory we have considered thus far assumes that chemical reactions are so rapid that chemical equilibrium prevails locally at all points in the gas mixture. If rates are slower, heat conduction decreases and

approaches the frozen value as the rates approach zero. A general expression has been derived (57) for the apparent thermal conductivity of reacting mixtures in which a single reaction proceeds at a finite rate. In contrast to systems in which reaction rates are either very high or very low, it is found that heat conduction depends on the geometry and scale of the system, as well as the catalytic activity of the surfaces and the gas phase reaction rate.

#### THE MODERATELY DENSE GAS

As we have already discussed, the theory for the transport properties of dilute monatomic gases is based on the Chapman-Enskog solution of the Boltzmann equation. If the intermolecular potential is known, the transport coefficients can be obtained in terms of binary collision integrals (equations (5)-(7)).

In the case of the moderately dense gas modern statistical mechanical theory tries to account, in turn, for the effects of binary collisions, then triple collisions, then quadruple collisions, etc. Such an approach was initiated by Bogoliubov (58).

It is well known that the equation of state of a gas can be represented by the virial expansion:

$$\frac{PV}{RT} = 1 + B\rho + C\rho^2 + \dots \quad (27)$$

In this series the second term arises from interactions between pairs of molecules, the third from interactions between clusters of three molecules,

etc. Until recently it was generally believed that the transport properties could also be expanded in a power series in density

$$\eta = \eta_0 [1 + B_\eta \rho + C_\eta \rho^2 + \dots] \quad (28)$$

$$\lambda = \lambda_0 [1 + B_\lambda \rho + C_\lambda \rho^2 + \dots] \quad (29)$$

because such an expansion was implicit in the theory of Bogoliubov. (Here  $\eta_0$  and  $\lambda_0$  are the low density values.)

However, detailed examination of the quadruple collision integrals which determine the coefficients  $C_\eta$  and  $C_\lambda$  indicates that they become infinite as the density approaches zero. These divergent coefficients were predicted by estimating the probability of the relevant collision events (59)-(62); they were later confirmed by explicitly evaluating corresponding terms for the transport coefficients of a two-dimensional gas of rigid disks (63)-(65). (For the two-dimensional gas the divergence occurs in the  $B_\eta$  and  $B_\lambda$  terms.) It is found that the leading term in  $C_\eta$  and  $C_\lambda$  is proportional to the logarithm of the mean free path. As the density approaches zero, the mean free path tends toward infinity; this is the source of the divergence in  $C_\eta$  and  $C_\lambda$ . Since at low density the mean free path is inversely proportional to the density it was suggested that  $C_\eta$  and  $C_\lambda$  be replaced by  $C_\eta \ln \rho + D_\eta$  and  $C_\lambda \ln \rho + D_\lambda$  (60)-(64). Consequently, equations (28) and (29) are replaced by

$$\eta = \eta_0 [1 + B_\eta \rho + C_\eta \rho^2 \ln \rho + D_\eta \rho^2 + \dots] \quad (30)$$

and

$$\lambda = \lambda_0 [1 + B_\lambda \rho + C_\lambda \rho^2 \ln \rho + D_\lambda \rho^2 + \dots]. \quad (31)$$

This conjecture has been supported by further theoretical studies (61),



(62) and (66). The nature of the succeeding terms in equations (30) and (31) is not known; it has been proposed that they include products of powers of  $\rho$  and  $\ln \rho$  (60), (67).

A recent analysis by Hanley, McCarty, and Sengers (68) suggests that equations (30) and (31) may be a better representation of experimental data than equations (28) and (29). Their procedure, discussed in detail for the case of heat conductivity data of neon (69), is as follows: first they fit the data to a linear equation, corresponding to the first two terms of equation (29) or (31),

$$\lambda = \lambda_0 [1 + B_\lambda \rho]. \quad (32)$$

They start by obtaining a least squares fit of six to eight data points in the density range up to 40 Amagat\*. They then consider successively larger numbers of data points, ultimately to a density of 120 Amagat, and observe that the coefficients  $\lambda_0$  and  $B_\lambda$  do not change significantly nor does the standard deviation of the least squares fit change. They conclude that equation (32) is consistent with the experimental data up to 120 Amagat.

Above 120 Amagat deviations from equation (32) occur; the standard deviation increases and the coefficients  $\lambda_0$  and  $B_\lambda$  begin to drift. At this point a quadratic term is added

$$\lambda = \lambda_0 [1 + B_\lambda \rho + C_\lambda \rho^2]. \quad (33)$$

Equation (33) is then fit to the data, starting with about 15 points in

---

\* The density in Amagat is the ratio of the actual density to the density at 0°C and 1 atmosphere.

the density range 0-200 Amagat. The density range is again increased, up to 440 Amagat, with no significant changes in the coefficients  $\lambda_0$ ,  $B_\lambda$ , and  $C_\lambda$ . However, the coefficient  $B_\lambda$  is 8-17% smaller than the value obtained in the linear range to 120 Amagat. This indicates that equation (33) is not consistent with the experimental data.

Next they consider the cubic equation,

$$\lambda = \lambda_0 [1 + B_\lambda \rho + C_\lambda \rho^2 + D_\lambda \rho^3], \quad (34)$$

and repeat the procedure, starting with the range 0-560 Amagat and extending it to 800 Amagat. Again the important result is that  $B_\lambda$  is smaller than the fit in the linear range, so that equation (34) is not consistent with the data.

These results are suggestive, but do not prove that equation (29) is incorrect; it is possible that in the density interval to 800 Amagat the data should be fit to a higher order polynomial. (However if a higher order polynomial is required it is not possible to obtain meaningful values of any of the coefficients from the experimental data.)

Finally, Hanley, McCarty, and Sengers (68) consider the equation

$$\lambda = \lambda_0 [1 + B_\lambda \rho + C_\lambda \rho^2 \ln \rho + D_\lambda \rho^2] \quad (35)$$

obtained by truncating equation (31). Equation (35) is fit to the data, starting in the range 0-240 Amagat. The density range can be extended to 720 Amagat without significant changes in the coefficients or increase in standard deviation. In contrast to the polynomial fits (equations (33) and (34)),  $B$  is the same as the value obtained in the linear range to 120 Amagat, within the standard deviation. Thus equation (35) is consistent

with the experimental data. Hanley, McCarty, and Sengers (68) conclude that their analysis yields meaningful values for the first density coefficient  $B_\lambda$ . They have applied this sort of analysis to viscosity and thermal conductivity data on a number of other gases.

These results would seem to have bearing on the problem of correlating the properties of steam; Weinstock (61) indicates that the considerations leading to equations (30) and (31) are not limited to molecules with central force laws. Hence these results should also apply to highly polar gases such as steam. Experimental thermal conductivity data should be correlated using equation (35) and viscosity data using the analogous expression

$$\eta = \eta_0 [1 + B_\eta \rho + C_\eta \rho^2 \ln \rho + D_\eta \rho^2]. \quad (36)$$

If more elaborate equations are required further empirical terms can be added.

Let us turn now to the question of the theoretical prediction of the coefficients  $B_\eta$  and  $B_\lambda$  which requires the evaluation of triple collision integrals. Thus far these triple collision integrals have evaluated only for a gas of rigid elastic spheres (70). However there have been several attempts to develop expressions for  $B_\eta$  and  $B_\lambda$  by introducing various approximations. The first such theory was that of Enskog for a dense gas of rigid elastic spheres (71). Enskog's values for the triple collision contribution to first density corrections agree with Senger's calculations to within five percent although there is at least the suggestion that this may be fortuitous.

Hoffman and Curtiss have generalized the Enskog approach to include the effect of soft potentials (72), (73) and have evaluated the first density corrections for the Lennard-Jones (12-6) potential (74). This potential has an attractive well which leads to both bound and unbound two-particle trajectories. Their calculations do not consider the bound states, so that their results can be meaningful only at high temperatures where bound states are not important.

At high temperatures their predictions are in reasonable accord with experimental data for the noble gases. In particular, they find that  $B_\eta$  is negative whereas  $B_\lambda$  is positive in the high temperature limit. At low temperatures their results do not agree with experiment, presumably due to neglect of bound states.

Because Enskog's approximation of the triple collision contribution is in reasonable accord with Sengers results (70) there is at least the hope that the Hoffman and Curtiss (74) calculations are good approximations to what might be obtained by a truly rigorous approach.

Another approach for approximating  $B_\eta$  and  $B_\lambda$  is more promising for use at low temperatures; the initial pressure dependence is assumed to arise from molecular association, and in particular, a mixture of monomers and dimers. The first treatment of this kind was due to Storgryn and Hirschfelder (75), and more recently Kim and Ross have carried out a similar analysis for viscosity (76), and, with Flynn, for thermal conductivity (77). The treatments of reference (75) and refs. (76), (77) differ principally in the way the equilibrium constant for the monomer-dimer

equilibrium is obtained. Hirschfelder and Storgryn (75) consider bound states and metastable dimer states while Kim and Ross (76) also consider quasidimers; these are pairs of molecules in orbiting collisions. (They show that the lifetimes of such pairs is large compared to collision times.) Thus triple collisions in both theories are replaced by binary collision between monomers and dimers.

Both theories assume a Lennard-Jones (12-6) potential and it turns out that the computed values of  $B_T$  and  $B_\lambda$  are sensitive to the force law assumed for the monomer-dimer interaction; consequently the force constant for this interaction was adjusted to obtain good agreement with experiment. Hence these theories may be helpful in predicting the density behavior for molecules obeying a Lennard-Jones potential, but they cannot make predictions for molecules obeying very different force laws in the complete absence of experimental data.

Are any of these theories helpful in predicting and correlating the properties of steam? The theory of Hoffman and Curtiss (74) might be helpful at high temperature, provided the intermolecular potential for steam can be approximated by a Lennard-Jones (12-6) potential. However, we have already seen that the more sophisticated Stockmayer potential does not do a good job of correlating the high temperature, low density viscosity of steam - see figure 4. In view of this failure it would seem fortuitous if the results of Hoffman and Curtiss (74) turn out to be applicable to steam.

Barua and Das Gupta (78) have applied the Storgryn-Hirschfelder type of analysis to the viscosity of steam. They seem to be able to rationalize

the experimental observation of Kestin and Richardson (17) that below about 315°C the viscosity of steam decreases with increasing pressure. Das Gupta and Barua (79) have considered the analogous problem of the thermal conductivity of steam. In this case there are inconsistencies amongst experimental data on the density dependence of the heat conductivity, so a meaningful comparison with experiment is not possible.

To sum up, theories for predicting the coefficients  $B_1$  and  $B_2$  are not developed to the point where they can be applied to steam. It seems reasonable that the Kim-Ross type of analysis (76), (77) can be used to obtain a qualitative understanding and rationalization of trends observed experimentally.

#### THE CRITICAL REGION

The critical region is a region where many properties show anomalous behavior. For example, the isothermal compressibility and the coefficient of thermal expansion become infinite at the critical point. The specific heat at constant pressure  $C_p$  is related to the compressibility so it diverges also. The compressibility and  $C_p$  diverge approximately as  $|T - T_c|^{-4/3}$  (80). Even the specific heat at constant volume is weakly divergent. In view of these anomalies in the equilibrium properties we should be alert to the possibility of analogous behavior in the transport coefficients.

Let us first consider the viscosity. Naldrett and Maass (81) were the first to investigate the viscosity of carbon dioxide in the critical

region in detail. (Carbon dioxide is a favorite subject of study because of its convenient critical temperature of  $31.0^{\circ}\text{C}$ .) When their data at  $31.1^{\circ}\text{C}$  are plotted as a function of density there appears to be a small anomalous increase in the viscosity near the critical density - see figure 11. Naldrett and Maass (81) used an oscillating disc viscometer. On the other hand, Michels, Botzen and Schuurman (82) using a capillary viscometer found a much larger anomaly, a factor of 2 at  $31.1^{\circ}\text{C}$  (not shown in figure 11). The capillary method is not suited to the critical region; because of the large compressibility there is a large density gradient in the capillary. To resolve the discrepancies between references (81) and (82) Kestin, Whitelaw, and Zien (83) reinvestigated using an oscillating disc instrument. Their data (figure 11) indicate that any anomalous increase in viscosity is much smaller than reported by Michels and coworkers. At  $31.1$  they found an anomalous increase of about the same amount as reported by Naldrett and Maass. At  $34.1^{\circ}\text{C}$ , only one percent above the absolute critical temperature, the anomaly has completely vanished - see the dashed curve in figure 11.

The significance of these small experimental anomalies in viscosity is not clear at this time (84). The effect may be merely a consequence of experimental difficulties near the critical point. On the other hand a recent theoretical study by Kadanoff and Swift (85) suggests that the viscosity at the critical point is either weakly divergent or strongly cusped.

We turn now to the heat conductivity. There has been controversy in

the past as to the presence or absence of an anomalous increase in the thermal conductivity in the critical region (84), (86). However, it now seems definite that there is an anomaly and that the heat conductivity diverges approximately as  $|T-T_c|^{-2/3}$ .

The first detailed survey of the critical region for carbon dioxide was due to Guildner (87), (88). He used a concentric cylinder apparatus and was not able to avoid heat transport due to natural convection. However, by making measurements with various temperature differences and extrapolating to  $\Delta T = 0$  he concluded that there is a pronounced anomaly in the thermal conductivity. This conclusion was confirmed by the painstaking work of Michels, Sengers, and van der Gulik (89)-(91) who used a parallel plate apparatus and thus avoided problems due to natural convection. These measurements are the most extensive and convincing direct demonstration of the heat conductivity anomaly. However, the effect has since been observed for other gases including ammonia (92), (93), sulfur hexafluoride (94), methane (95) and argon (96).

The data of Michels, Sengers, and van der Gulik are shown in figure 12, as plots of thermal conductivity against density for several isotherms. The maximum at  $31.2^\circ\text{C}$  and critical density is about six times as large as would be predicted from the smooth dashed curve connecting low and high density data. This temperature is less than  $0.2^\circ\text{C}$  above the critical point. As the temperature is raised the anomaly decreases rapidly. At  $32.1^\circ\text{C}$ , the heat conductivity is only about 40% as large as at  $31.2^\circ$  and when the temperature is raised to  $75^\circ\text{C}$  the anomaly is barely perceptible.



The anomaly occurs over a narrow range of pressures. For example, at  $31.2^\circ$  the density doubles from 0.3 to 0.6 gm/cm<sup>3</sup> when the pressure is raised about three percent from 71.5 to 73.9 atmospheres. Thus the heat conductivity anomaly may be missed entirely unless measurements are made at pressures corresponding very closely to critical density.

Very recently the thermal conductivity anomaly has been verified by an entirely different experimental technique, namely laser light scattering. An abbreviated discussion of this subject has been presented by Sengers and Levelt Sengers (97) and a more exhaustive review is given by McIntyre and Sengers (98). Very briefly, the spectrum of light scattered by fluids consists of a central Rayleigh line at the wave length of the light source and two symmetrically displaced Brillouin lines. The scattering is caused by fluctuations in the fluid. The Brillouin lines are due to fluctuations in pressure at constant entropy, that is sound waves. Sound waves propagate at the sound speed which leads to the Doppler displacement of the Brillouin lines from the source frequency. The width of the Brillouin lines is a measure of the sound attenuation. The central Rayleigh line is due to fluctuations of entropy at constant pressure. These do not propagate but decay by heat conduction. Consequently the width of the Rayleigh line is proportional to the thermal diffusivity,  $\lambda/\rho c_p$ . Finally, the ratio of the intensity of the Rayleigh lines to the sum of the intensities of the Brillouin lines is  $(C_p/C_v)-1$ . In the critical region  $C_p$  diverges much faster than  $C_v$ , so that most of the intensity of the scattered light goes into the Rayleigh line.

Thus if one can measure the width of the Rayleigh line and knows the behavior of  $C_p$ , one has another method of determining thermal conductivity. This method does not require imposition of macroscopic temperature gradients so that there are no disturbances due to natural convection and the critical point can be approached as closely as desired.

However, until very recently it has not been possible to measure Rayleigh line width in the critical region since the line widths are far too narrow to be measured by conventional spectroscopic methods. With the advent of the laser, however, new high resolution spectroscopic techniques are possible so that the scattered spectrum can be measured with remarkable accuracy.

The first measurements of Rayleigh line width near the critical point were those of Ford and Benedek (99), (100) on sulfur hexafluoride. Swinney and Cummins (101) have measured the thermal diffusivities of carbon dioxide along the critical isochore from 0.02 to 5.3°C above the critical temperature and also along the gas and liquid sides of the coexistence curve. Their results on the critical isochore are shown in figure 13 along with the data of Seigel and Wilcox (102), obtained by the same technique. The open squares are thermal diffusivities calculated from experimental heat conductivities combined with equation of state data (103). The slope of the line is 0.73 so that the thermal diffusivity is proportional to  $|T-T_c|^{0.73}$ . Along the liquid side of the coexistence line Swinney and Cummins find the thermal diffusivity proportional to  $|T-T_c|^{0.72}$  and along the gas side it varies at  $|T-T_c|^{0.66}$ .

Osmundson and White (104) have also measured Rayleigh line widths in carbon dioxide and report that at constant density they are proportional to  $|T-T_c|^{2/3}$ . Saxman and Benedek (105) have studied sulfur hexafluoride and find along the coexistence curve the line width proportional to  $|T-T_c|^{0.64}$ . But along the critical isochore above the critical point they find line width proportional to  $|T-T_c|^{1.27}$ . This last result is in disagreement with all the data on carbon dioxide and merits further investigation.

Thus the indication is that in the critical region the thermal diffusivity tends toward zero approximately as  $|T-T_c|^{2/3}$ . Since  $C_p$  diverges as  $|T-T_c|^{-4/3}$ , this implies that the thermal conductivity must also tend toward infinity and be proportional to  $|T-T_c|^{-2/3}$ . This is in accord with the recent theoretical investigation of Kadanoff and Swift (85) which indicates that the thermal conductivity would diverge in this same fashion on the critical isochore and the coexistence curve.

Thus it seems well-established that the heat conductivity does indeed have a pronounced anomaly in the critical region. It has been suggested (90), (91) that this may be due to the presence of large clusters of molecules in the gas. In the presence of a temperature gradient these clusters tend to form in the cool regions and diffuse to the warm regions where they break up and absorb heat in the process. This is quite analogous to the situation in the dissociating gas which we have already discussed. Indeed, we can apply the theory of heat conduction in a chemically reacting to predict heat conductivities of the right order of magnitude, and by an ad hoc adjustment the theory can be made nearly quantitative.

We begin by imagining that the heat conductivity consists of two parts

$$\lambda = \lambda_f + \lambda_r. \quad (37)$$

Here  $\lambda_r$  represents the contribution due to diffusion and dissociation of clusters whereas  $\lambda_f$  represents the rest of the heat conductivity—the dashed curve in figure 12.

Of course there must be a whole spectrum of cluster sizes. However, for simplicity we will assume that the gas can be approximated as consisting of a monomer and a single large cluster of  $n$  monomer units. In other words, we assume a single reaction



We will relate the thermal conductivity to other experimental quantities such as the specific heat and the compressibility. In this way we can hope that some of the crude aspects of the model will be ameliorated.

For a gas with a single dissociation we have already seen that

$$\lambda_r = \frac{D_{1n}P}{RT} \frac{\Delta H^2}{RT^2} \frac{x_1 x_n}{(x_1 + n x_n)^2} \quad (39)$$

(see equation (26)). Here  $x_1$  and  $x_n$  are the mole fractions of the monomers and clusters while  $D_{1n}$  is the binary diffusion coefficient between monomers and clusters.

The specific heat of such a reacting gas is also augmented by an amount (5)

$$c_p = \frac{1}{\rho} \frac{P}{RT} \frac{\Delta H^2}{RT} \frac{x_1 x_n}{(x_1 + n x_n)^2}. \quad (40)$$

By combining equations (39) and (40) we find

$$\lambda_r = \rho D_{1r} c_{p_r} \quad (41)$$

Equation (41) is also correct for a system involving multiple equilibria provided all the binary diffusion coefficients between the various molecular species are numerically equal. (This follows by inspection of the theoretical expressions for  $c_{p_r}$  (106) and  $\lambda_r$  (52).)

Let us now rewrite equation (41) as

$$\lambda_r = \rho D \left( \frac{D_{1n}}{D} \right) c_{p_r} \quad (42)$$

where  $D$  is the self diffusion coefficient. Experiment indicates that there is no anomaly in  $D$  in the critical region. Thus Trappeniers and Oosting (107) find that the self diffusion coefficient of methane in the critical region is within 5% of the low density value, and DePaz (108) has obtained a similar result for argon. Hence we will take  $D$  as the low density value, given by Chapman-Enskog Theory, equation 3. From the Chapman-Enskog expressions for the binary and self diffusion coefficients we obtain

$$\frac{D_{1n}}{D} = \frac{\sigma_{11}^2 \Omega_{11}^{(1,1)*}}{\sigma_{1n}^2 \Omega_{1n}^{(1,1)*}} \sqrt{\frac{1}{2} \left( 1 + \frac{1}{n} \right)}. \quad (43)$$

Here  $\sigma_{11}^2 \Omega_{11}^{(1,1)*}$  is the diffusion cross section for the monomer-monomer interaction while  $\sigma_{1n}^2 \Omega_{1n}^{(1,1)*}$  is the corresponding cross section for the monomer-cluster interaction.

We can make a crude estimate of the ratio of cross sections as follows: If we assume the molecules behave as rigid spheres then  $\Omega_{11}^{(1,1)*}$  and

$\Omega_{1n}^{(1,1)*}$  are by definition unity. We also would expect that the volume of the cluster should be proportional to the number of particles it contains,

$$\frac{\sigma_n^3}{\sigma_1^3} = bn \quad (44)$$

where  $\sigma_n$  is the diameter of the cluster and  $b$  is a factor related to the geometry and density of the cluster. For example, if the cluster is spherical and the density corresponding to a closest packing of spheres, (coordination number 12) 74.05% of the volume is occupied and  $b = 0.7405^{-1} = 1.35$ . On the other hand, if the cluster is still spherical, but has the more open structure of a diamond lattice (coordination number 4)  $b = 3$ . Assuming the usual combination rule,  $\sigma_{1n} = \frac{1}{2}(\sigma_1 + \sigma_n)$ ,

$$\frac{D_{1n}}{D} = \left[ \frac{2}{1 + (bn)^{1/3}} \right]^2 \left[ \frac{1}{2} \left( 1 + \frac{1}{n} \right) \right]^{\frac{1}{2}}. \quad (45)$$

Thus we can predict the thermal conductivity anomaly from equations (42), (45) and the specific heat, provided we can establish values of  $b$  and  $n$ .

As to the cluster size  $n$ , the most obvious course is to require that the gas density and compressibility are appropriate for an ideal gas mixture of the monomer and cluster. Thus

$$\rho = \frac{PM}{RT} = \frac{PM_1}{RT} (x_1 + nx_n) \quad (46)$$

subject to the equilibrium condition

$$K_p = \frac{p_1^n}{p_n} = \frac{x_1^n}{x_n} p^{n-1}. \quad (47)$$

Where  $p_1$ ,  $p_n$  are the partial pressures of the monomer and cluster,  $P$  is the total pressure, while the equilibrium constant  $K_p$  is a function of temperature alone.

After straightforward partial differentiation followed by considerable algebra, we find that

$$n = \frac{\frac{RT}{PV} \left( \frac{\partial \ln p}{\partial \ln P} \right)_T - 1}{1 - \frac{PV}{RT}}. \quad (48)$$

In figure 14 experimental thermal conductivities of carbon dioxide are compared with values calculated from equations (37), (42) and (45). The normal contribution to the heat conductivity,  $\lambda_f$ , was taken from the dashed curve of figure 12. The calculations have been made for  $b = 1.35$  (closest packing, coordination number 12) and  $b = 3$  (diamond lattice). There is qualitative agreement with experiment; predicted conductivities are of the right order of magnitude and show the correct density dependence. If one believes the model, it would seem that the larger clusters are more compact and the smaller ones more loosely organized.

What is the asymptotic behavior as  $T \rightarrow T_c$ ? The compressibility diverges as  $|T - T_c|^{-4/3}$  so that  $n$  will diverge in the same fashion and  $D_{1n}/D$  will tend to zero as  $|T - T_c|^{8/9}$ . The specific heat also diverges as  $|T - T_c|^{-4/3}$ , so that we predict that the heat conductivity will diverge as  $|T - T_c|^{-4/9}$ . But we have already seen that the conductivity diverges more rapidly, as  $|T - T_c|^{-2/3}$ .

We can apply an ad hoc fix by assuming that  $b$  varies as  $n^{-1/4}$ , which gives the correct asymptotic behavior. Consequently we replace equation (45) by

$$\frac{D_{in}}{D} = \left[ \frac{2}{1 + (2.1)n^{1/4}} \right]^2 \left[ \frac{1}{2} \left( 1 + \frac{1}{n} \right) \right]^{\frac{1}{2}}, \quad (49)$$

where the constant 2.1 has been chosen to give a good fit to the experimental data.

Calculations for which equation (45) was replaced by equation (49) are compared with experiment in figure 15. The agreement between theory and experiment is now rather good. The most serious discrepancy is in the vicinity of the maximum in the 31.2°C and there is an indication that the experimental data may be somewhat too high in that region - see figure 13. Thus equations (42), (48) and (49) would appear to provide a reasonable means of estimating the anomalous increase in heat conductivity in the critical region.

This result should be directly applicable to steam. The skeleton tables do not recognize any heat conductivity anomaly in the critical region. Yet there is no reason to believe that steam is any way unusual in this regard. Indeed, there seems to be nothing unusual about the thermodynamic anomalies of steam in the critical region. Steam behaves very much like other gases (109). Specifically, equations (42), (48) and (49) should be directly applicable to steam. In the absence of experimental data these equations can be used to estimate the thermal conductivity anomaly from the specific heat and compressibility. The quantity  $\rho D$  can be estimated from



the low density viscosity near the critical temperature:

$$\frac{\rho D}{\eta} = \frac{6}{5} \frac{\Omega_L(2,2)^*}{\Omega_L(1,1)^*} \approx 1.32. \quad (50)$$

This is a good approximation for most realistic intermolecular force laws.

The critical anomaly in viscosity if any, seems to be small and can be ignored for practical engineering purposes.

### THE LIQUID STATE

The theory of the liquid state is an area of very active research at the present time, but as yet we have not achieved a truly quantitative description even for simple fluids without internal structure - in other words, the noble gases. Thus in introducing an article on approximate theories of the liquid state de Boer and Uhlenbeck (110) assert "In our opinion the article shows clearly how much, or perhaps one should say how little, one knows at present about the liquid state: the theory of liquids is still one of the unsolved problems in statistical mechanics."

The article in question concerned equilibrium properties. One might suspect that the situation with respect to the transport coefficients would be no better. This suspicion is confirmed by a statement made by Zwanzig (111) in reviewing a new book on the theory of simple dense fluids:

"Numerical calculations of viscosity, thermal conductivity, and diffusion are compared with experiment, and agreement is typically no better than within a factor of two. (This may be not much better than one can get from dimensional analysis and the simplest of physical pictures.)" It might be added that this modest result is achieved at the expense of a

rather considerable numerical effort.

This is the situation with regard to simple fluids. Thus it is obvious that theory has virtually nothing to offer in describing water. The water molecule has internal energy states and a large dipole moment as well. These will certainly lead to much further complexity.

#### CONCLUDING REMARKS

Statistical mechanical theories of transport properties can help in correlating and selecting properties of steam under many conditions where experimental data are available. And theory can make reasonable predictions for some regimes in which there is no data.

The theory for the dilute monatomic gas is well developed and applies well to the noble gases. Thus one can predict heat conductivities of these gases from their viscosities. Certain discrepancies amongst various experimental determinations of the viscosity of steam can be in a large measure resolved by reexamining the data of investigators who also measured the viscosity of argon. In this fashion it is possible, in essence, to recalibrate their apparatus based on recent and more reliable viscosities for this gas. A similar procedure reduces discrepancies in the case of the heat conductivity also. The theory for polyatomic gases is not yet able to make predictions reliable enough to choose among conflicting experimental data.

There are no data on the properties of steam at temperatures above  $2000^{\circ}\text{C}$  where dissociation occurs. Here theory must be used and an order of magnitude increase in the heat conductivity due to dissociation reactions

is to be expected. Predicted properties may be in error by roughly twenty percent.

Turning to the moderately dense gas, recent theoretical developments indicate the correct mathematical form for the first few terms in the series expansion for the transport coefficients as a function of density. These include, first a constant (the dilute gas viscosity or heat conductivity), next a term proportional to density followed by terms proportional to  $\rho^2$  and  $\rho^2 \ln \rho$ . The nature of higher terms is not known. This form should be applied in correlating properties of steam. On the other hand, theory is not yet able to predict the values of the coefficients of the terms in these density expansions.

In the critical region there is an anomaly in the heat conductivity. It tends toward infinity as the critical point is approached. A simple theory based on the diffusion and dissociation of large clusters can be adjusted to make quantitative predictions of this heat conductivity anomaly for steam. (There is as yet no reliable experimental data on steam very close to the critical point.)

The theory of the liquid state has not advanced sufficiently to be useful for predicting or correlating the properties of water.

## ACKNOWLEDGMENTS

I am very much indebted to Professor Jan V. Sengers of the University of Maryland for invaluable information concerning the dense gas and critical regions. Indeed, my discussion of the dense gas is taken rather directly from two of his papers (68) and (86). Thanks are also due to Professors Joseph Kestin and Edward A. Mason of Brown University, for helpful discussions concerning the available experimental data on the transport coefficients of steam and the theory of the low density transport properties.

## REFERENCES

1. S. Chapman and T. G. Cowling, The Mathematical Theory of Non-Uniform Gases, Cambridge University Press, London & New York, 2nd Ed., 1952.
2. J. O. Hirschfelder, C. F. Curtiss, and R. B. Bird, Molecular Theory of Gases and Liquids, John Wiley & Sons, Inc., New York, 2nd printing, 1964.
3. Reference 2, p. 527.
4. P. E. Phillipson, Phys. Rev. 125, 1981 (1962).
5. E. A. Mason and L. Monchick in Advances in Chemical Physics, Vol. 12, Intermolecular Forces, J. O. Hirschfelder, ed., Interscience Publishers, New York, 1967, pp. 329-387.
6. E. A. Mason in Proceedings of the Fourth Symposium on Thermophysical Properties, J. R. Moszynski, ed., American Society of Mechanical Engineers, New York, 1968, pp. 21-29.
7. M. Trautz and H. E. Binkele, Ann. Physik 5, 561 (1930).
8. M. Trautz and R. Zink, Ann. Physik 7, 427 (1930).
9. V. Vasilescu, Ann. Physique 20, 292 (1945).
10. I. Amdur and J. Ross, Comb. Flame 2, 418 (1958).
11. I. Amdur and E. A. Mason, J. Chem. Phys. 22, 670 (1954).
12. R. DiPippo and J. Kestin in Proceedings of the Fourth Symposium on Thermophysical Properties, J. R. Moszynski, ed., American Society of Mechanical Engineers, New York, 1968, pp. 304-313.
13. F. A. Guevara, B. B. McInteer, and W. E. Wageman, cited in reference 14.
14. H. J. M. Hanley and G. E. Childs, Science 159, 1114 (1968).
15. C. F. Bonilla, S. J. Wang, and H. Weiner, Trans. Am. Soc. Mech. Engrs. 78, 1285 (1956).
16. A. S. Shifrin, Teploenergetika 6, (9), 22 (1959).
17. J. Kestin and P. D. Richardson, Trans. ASME, J. Heat Trans. 83C, 111 (1961).
18. J. Kestin and J. H. Whitelaw, Trans. ASME, J. Eng. Power 88A, 82 (1966).

19. B. Latto, Int. J. Heat Mass Trans. 8, 689 (1965).
20. H. Geier and K. Schäfer, Allgem. Wärmetech. 10, 70 (1961).
21. N. B. Vargaftik and N. Kh. Zimina, Teploenergetika 11 (12), 84 (1964); Thermal Engineering 11 (12), 114 (1964).
22. N. B. Vargaftik and N. Kh. Zimina, Teplofiz. Vysok. Temp. 2, 716 (1964); High Temperature 2, 645 (1964).
23. N. B. Vargaftik and N. Kh. Zimina, Teplofiz. Vysok. Temp. 2, 869 (1964); High Temperature 2, 782 (1964).
24. E. H. Kennard, Kinetic Theory of Gases, McGraw-Hill Book Co., New York, 1938, pp. 312-315.
25. B. Schramm and K. Schäfer, Ber. Bunsenges. Physik. Chem. 69, 110 (1965).
26. L. Monchick and E. A. Mason, J. Chem. Phys. 35, 1676 (1961).
27. E. A. Mason, J. T. Vanderslice, and J. M. Yos, Phys. Fluids 2, 688 (1959).
28. R. D. Nelson, Jr., D. R. Lide, Jr., and A. A. Maryott, Selected Values of Electric Dipole Moments for Molecules in the Gas Phase, National Standard Reference Data Series, National Bureau of Standards 10, Sept. 1, 1967.
29. H. Braune and R. Linke, Z. Physik. Chem. 148A, 195 (1930).
30. J. S. Rowlinson, Trans. Faraday Soc. 47, 120 (1951).
31. A. Eucken, Phys. Z. 14, 324 (1913).
32. A. R. Ubbelohde, J. Chem. Phys. 3, 219 (1935).
33. C. S. Wang Chang and G. E. Uhlenbeck, University of Michigan Report No. CM-681 (July 1951).
34. C. S. Wang Chang, G. E. Uhlenbeck, and J. de Boer, in Studies in Statistical Mechanics, Vol. 2, J. de Boer and G. E. Uhlenbeck, eds., North-Holland Publishing Co., Amsterdam, 1964, pp. 241-268.
35. N. Taxman, Phys. Rev. 110, 1235 (1958).
36. E. A. Mason and L. Monchick, J. Chem. Phys. 36, 1622 (1962).

37. H. Roesler and K. F. Sahm, J. Acoust. Soc. Am. 37, 386 (1965).
38. K. Yamada and Y. Fujii, J. Acoust. Soc. Am. 39, 250 (1966).
39. N. F. Sather and J. S. Dahler, J. Chem. Phys. 35, 2029 (1961).
40. N. F. Sather and J. S. Dahler, J. Chem. Phys. 37, 1947 (1962).
41. C. O'Neal, Jr. and R. S. Brokaw, Phys. Fluids 6, 1675 (1963).
42. C. E. Baker and R. S. Brokaw, J. Chem. Phys. 40, 1523 (1964).
43. C. E. Baker and R. S. Brokaw, J. Chem. Phys. 43, 3519 (1965).
44. C. E. Baker, J. Chem. Phys. 46, 2846 (1967).
45. R. A. Svehla, Thermodynamic and Transport Properties for the Hydrogen-Oxygen System, NASA Special Publication SP-3011.
46. Ref. 2, pp 531-2.
47. C. Muckenfuss and C. F. Curtiss, J. Chem. Phys. 29, 1293 (1958).
48. J. O. Hirschfelder, Sixth Symposium (International) on Combustion, Reinhold Publishing Corp., New York, 1957, p. 351.
49. J. O. Hirschfelder, Proceedings of the Joint Conference on the Thermodynamic and Transport Properties of Fluids, Institution of Mechanical Engineers, London, 1958, p. 133.
50. L. Monchick, A. N. G. Pereira and E. A. Mason, J. Chem. Phys. 42, 3241 (1965).
51. J. N. Butler and R. S. Brokaw, J. Chem. Phys. 26, 1636 (1957).
52. R. S. Brokaw, J. Chem. Phys. 32, 1005 (1960).
53. K. P. Coffin and C. O'Neal, Jr., NACA Tech. Note 4209, Feb. 1958.
54. R. S. Brokaw and R. A. Svehla, J. Chem. Phys. 44, 4643 (1966).
55. R. S. Brokaw, Planet. Space Sci. 3, 238 (1961).
56. E. U. Franck and W. Spalthoff, Naturwissenschaften 40, 580 (1953).
57. R. S. Brokaw, J. Chem. Phys. 35, 1569 (1961).

58. N. N. Bogoliubov, in Studies in Statistical Mechanics, Vol. I, J. de Boer and G. E. Uhlenbeck, eds., North-Holland Publishing Co., Amsterdam, 1962, pp. 5-118.
59. J. Dorfman and E. G. D. Cohen, Phys. Letters 16, 124 (1965).
60. J. Dorfman and E. G. D. Cohen, J. Math. Phys. 8, 282 (1967).
61. J. Weinstock, Phys. Rev. 140, A460 (1965).
62. R. Goldman and E. A. Frieman, J. Math. Phys. 8, 1410 (1967).
63. J. V. Sengers, Phys. Rev. Letters 15, 515 (1965).
64. J. V. Sengers, Phys. Fluids 9, 1685 (1966).
65. L. K. Haines, J. R. Dorfman and M. H. Ernst, Phys. Rev. 144, 207 (1966).
66. K. Kawasaki and I. Oppenheim, Phys. Rev. 139, A1763 (1966).
67. J. M. J. Van Leeuwen and A. Weyland, Phys. Letters 19, 562 (1965).
68. H. J. Hanley, R. D. McCarty and J. V. Sengers, to be published.
69. J. V. Sengers, W. T. Bolk and C. J. Stigter, Physica 30, 1018 (1964).
70. J. V. Sengers, in Lectures in Theoretical Physics, Vol. IX-C, Kinetic Theory, W. E. Brittin, ed., Gordon and Breach, New York, 1967, pp. 325-74.
71. Ref. 1, pp. 273-94 and Ref. 2, pp. 634-52.
72. D. K. Hoffman and C. F. Curtiss, Phys. Fluids 7, 1887 (1964).
73. D. K. Hoffman and C. F. Curtiss, Phys. Fluids 8, 667 (1965).
74. D. K. Hoffman and C. F. Curtiss, Phys. Fluids 8, 890 (1965).
75. D. E. Storgryn and J. O. Hirschfelder, J. Chem. Phys. 31, 1545 (1959).
76. S. K. Kim and J. Ross, J. Chem. Phys. 42, 263 (1965).
77. S. K. Kim, G. P. Flynn and J. Ross, J. Chem. Phys. 43, 4166 (1965).
78. A. K. Barua and A. Das Gupta, Trans. Faraday Soc. 59, 2243 (1963).
79. A. Das Gupta and A. K. Barua, Int. J. Heat Mass Transfer 10, 409 (1967).



80. M. E. Fisher, in Critical Phenomena, M. S. Green and J. V. Sengers, eds., National Bureau of Standards Miscellaneous Publication 273, Dec. 1, 1966, pp. 21-25.
81. S. N. Naidrett and O. Maass, *Canad. J. Res.* 18B, 322 (1940).
82. A. Michels, A. Botzen and W. Schuurman, *Physica* 23, 95 (1957).
83. J. Kestin, J. H. Whitelaw and T. F. Zien, *Physica* 30, 161 (1964).
84. J. V. Sengers, Reference 80, pp. 165-178.
85. L. P. Kadanoff and J. Swift, *Phys. Rev.* 166, 89 (1968).
86. J. V. Sengers, Proceedings of the Fourth Technical Meeting of the Society of Engineering Science.
87. L. A. Guildner, *Proc. Nat. Acad. Sci.* 44, 1149 (1958).
88. L. A. Guildner, *J. Res. NBS* 66A, 341 (1962).
89. A. Michels, J. V. Sengers and P. S. van der Gulik, *Physica* 28, 1201 (1962).
90. A. Michels, J. V. Sengers and P. S. van der Gulik, *Physica* 28, 1216 (1962).
91. J. V. Sengers, Thermal Conductivity Measurements at Elevated Gas Densities Including the Critical Region, Thesis, University of Amsterdam, 1962.
92. I. F. Golubev and V. P. Sokolova, *Teploenergetika* 11, (9), 64 (1964); *Thermal Engineering* 11, (9), 78 (1964).
93. D. P. Needham and H. Ziebland, *Int. J. Heat Mass Transfer* 8, 1387 (1965).
94. J. Lis and P. O. Kellard, *Brit. J. Appl. Phys.* 16, 1099 (1965).
95. V. P. Sokolova and I. F. Golubev, *Teploenergetika* 14, (4), 91 (1967); *Thermal Engineering* 14, (4), 123 (1967).
96. B. J. Bailey and K. Kellner, *Brit. J. Appl. Phys.* 18, 1645 (1967).
97. J. V. Sengers and A. Levelt Sengers, *Chem. and Eng. News* 46, (25), 104 (1968).

98. D. McIntyre and J. V. Sengers, in Physics of Simple Fluids, H. N. V. Temperley, J. S. Rowlinson and G. S. Rushbrooke, eds., North-Holland Publishing Co., Amsterdam, 1968, Ch. XI.
99. N. C. Ford, Jr. and G. B. Benedek, Phys. Rev. Letters, 15, 649 (1965).
100. N. C. Ford, Jr. and G. B. Benedek, Ref. 80, pp. 150-156.
101. H. L. Swinney and H. Z. Cummins, Phys. Rev. 171, 152 (1968).
102. L. Seigel and L. R. Wilcox, Bull. Am. Phys. Soc. 12, 525 (1967).
103. J. V. Sengers, Int. J. Heat Mass Transfer 8, 1103 (1965).
104. J. S. Osmundson and J. A. White, Bull. Am. Phys. Soc. 13, 183 (1968).
105. A. C. Saxman and G. B. Benedek, to be published; G. B. Benedek in Brandeis University Summer Institute in Theoretical Physics, 1966 Lectures, M. Chretien, S. Deser and E. P. Gross eds. Gordon and Breach, New York, 1968, Vol. 2.
106. R. A. Svehla and R. S. Brokaw, AIAA Journal 4, 182 (1966).
107. N. J. Trappeniers and P. H. Oosting, Phys. Letters 23, 445 (1966).
108. M. De Paz, in Proceedings of the Fourth Symposium on Thermophysical Properties, J. R. Moszynski, ed., Am. Soc. Mech. Engrs., New York, 1968, pp. 21-29.
109. J. M. H. Levelt Sengers, Paper presented at this Conference and submitted to Int. J. Heat & Mass Transfer.
110. J. de Boer and G. E. Uhlenbeck, in Studies in Statistical Mechanics, Vol. II, North-Holland Publishing Company, Amsterdam, 1964, Preface, p. VI.
111. R. Zwanzig, Science 160, 1102 (1968).

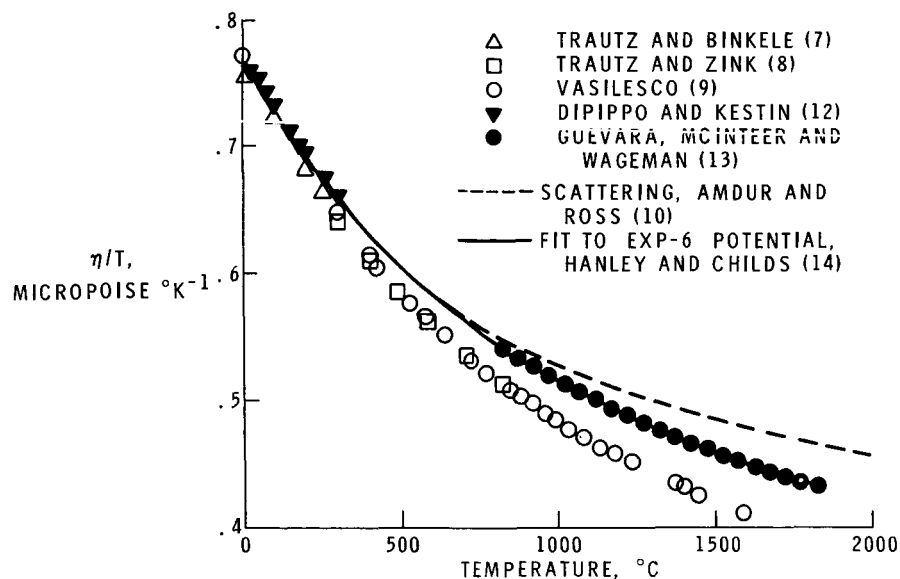


Figure 1. - Viscosity-temperature quotient for argon as a function of temperature.

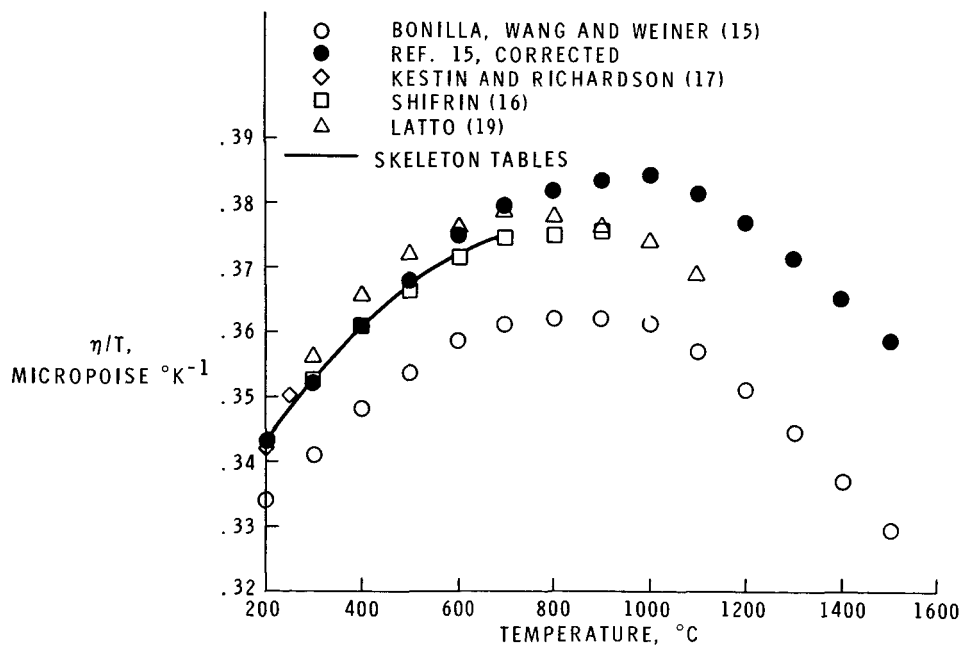


Figure 2. - Viscosity-temperature quotient for steam as a function of temperature.

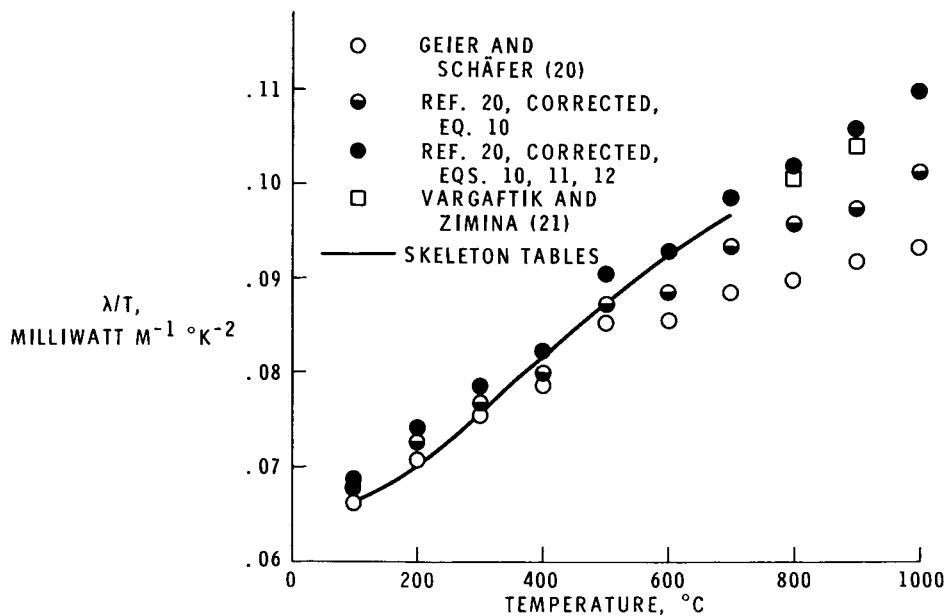


Figure 3. - Thermal conductivity-temperature quotient for steam as a function of temperature.

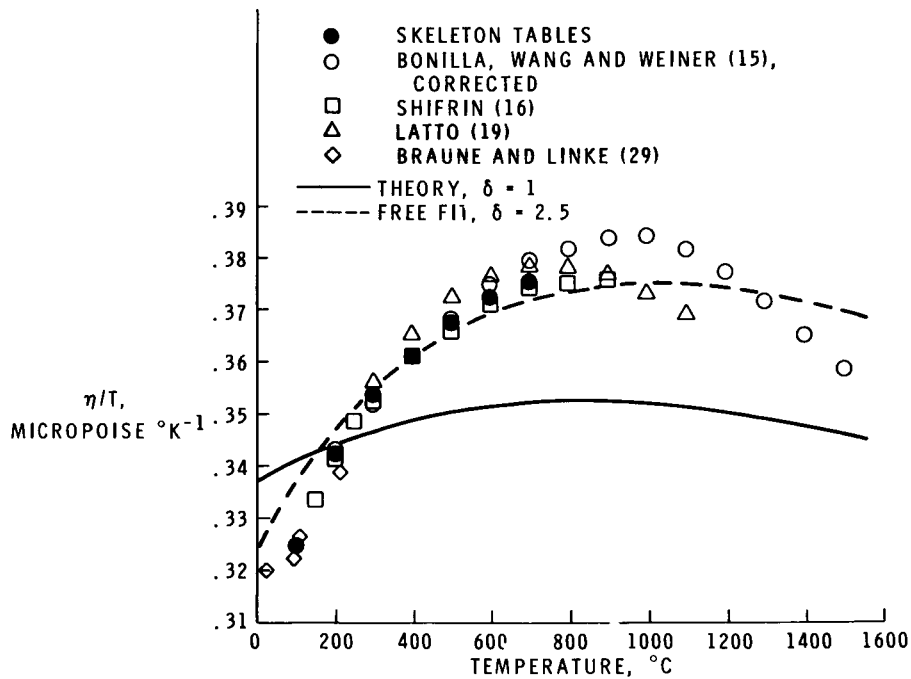


Figure 4. - Viscosity-temperature quotient for steam. Comparison of theory and experiment.

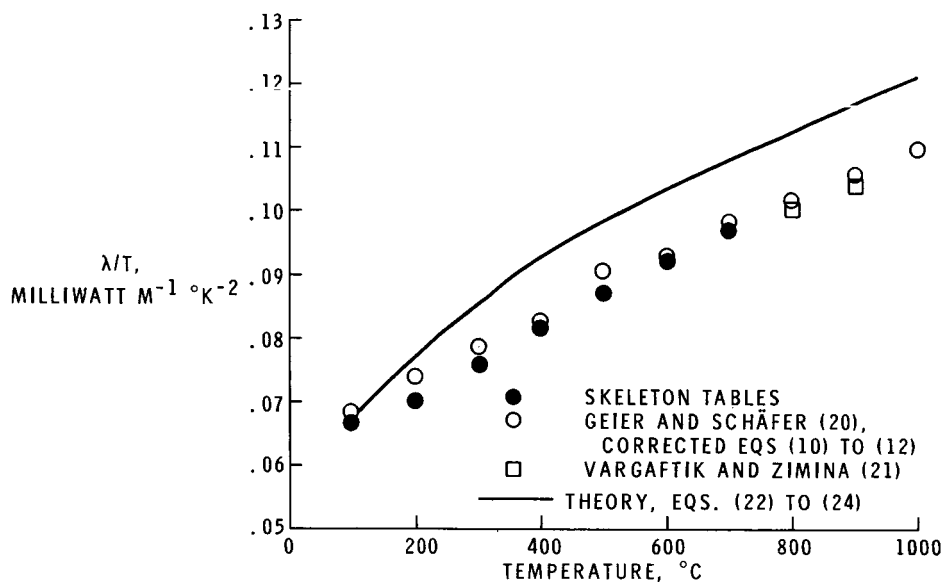


Figure 5. - Thermal conductivity-temperature quotient for steam. Comparison of theory and experiment.

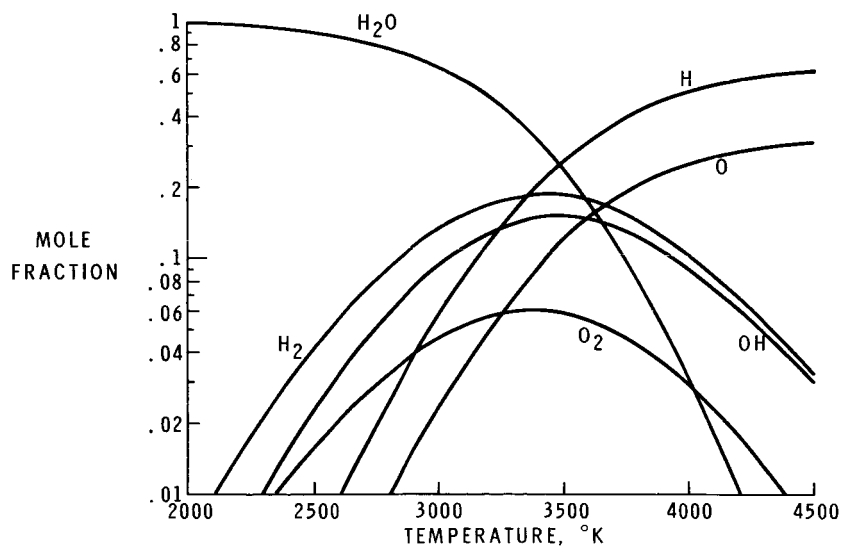


Figure 6. - Equilibrium composition of steam at one atmosphere as a function of temperature (Svehla, Ref. 45).

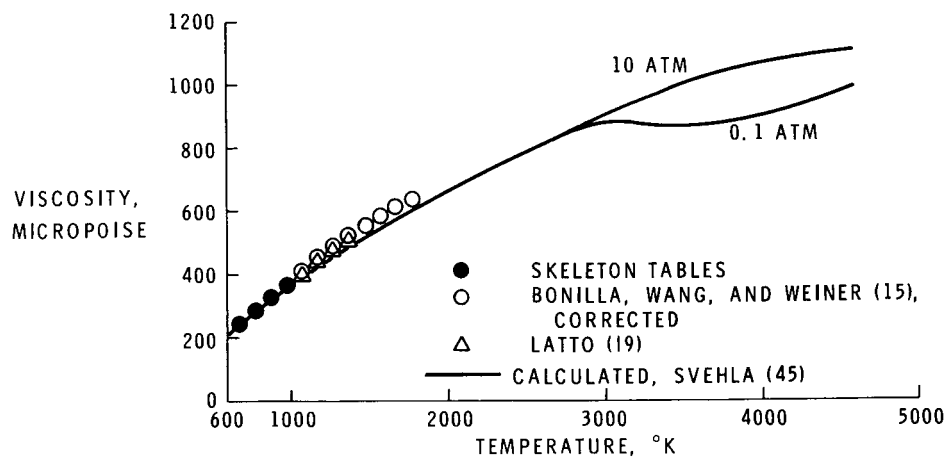


Figure 7. - Calculated viscosities of equilibrium steam at high temperatures.

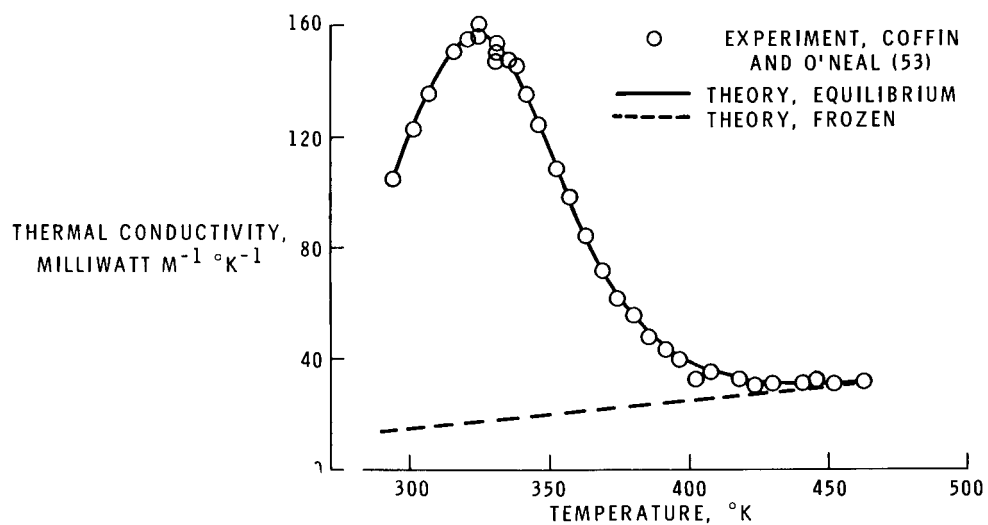


Figure 8. - Thermal conductivity of nitrogen tetroxide - nitrogen dioxide system. P = 1 atm.

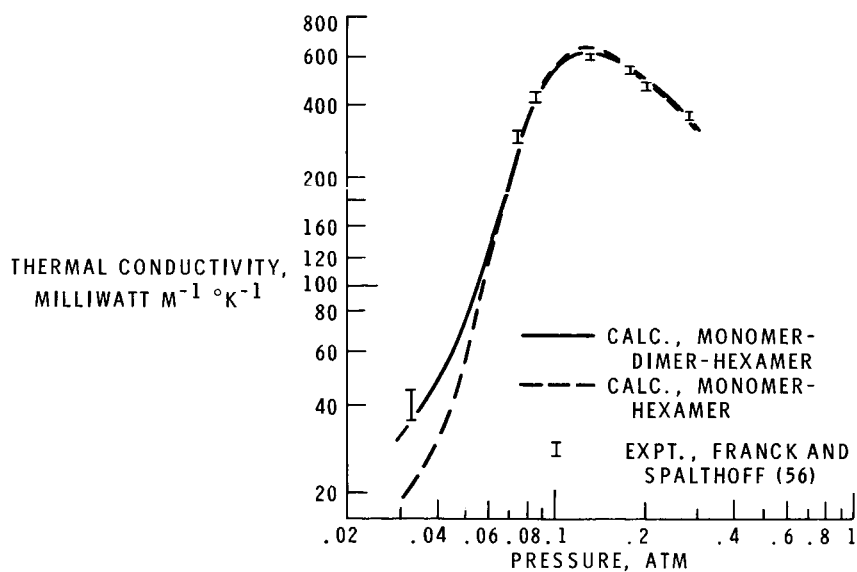


Figure 9. - Thermal conductivity of hydrogen fluoride vapor at 267.7° K.

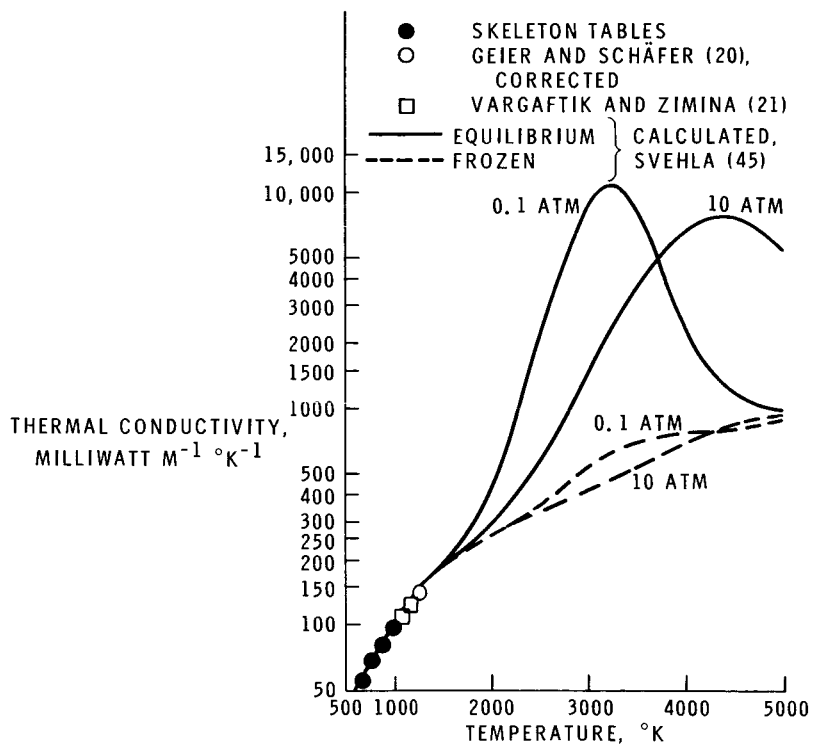


Figure 10. - Calculated thermal conductivities of equilibrium steam at high temperatures.

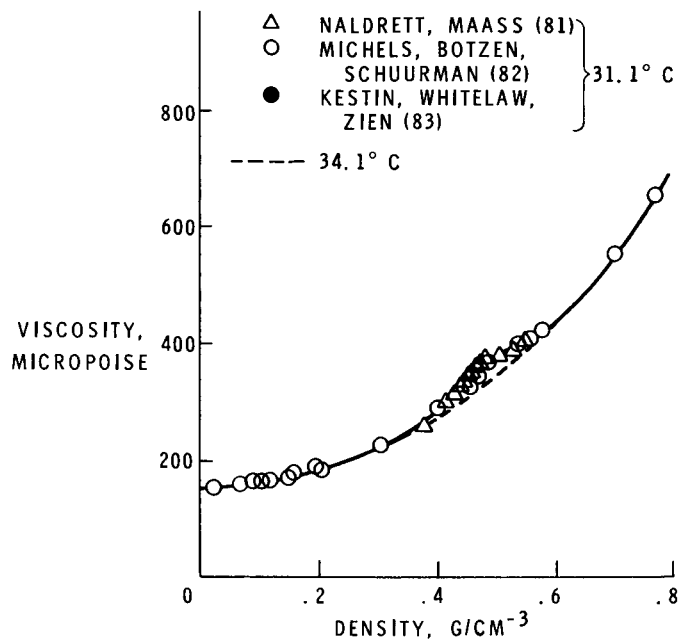


Figure 11. - The viscosity of CO<sub>2</sub> near the critical temperature as a function of density.

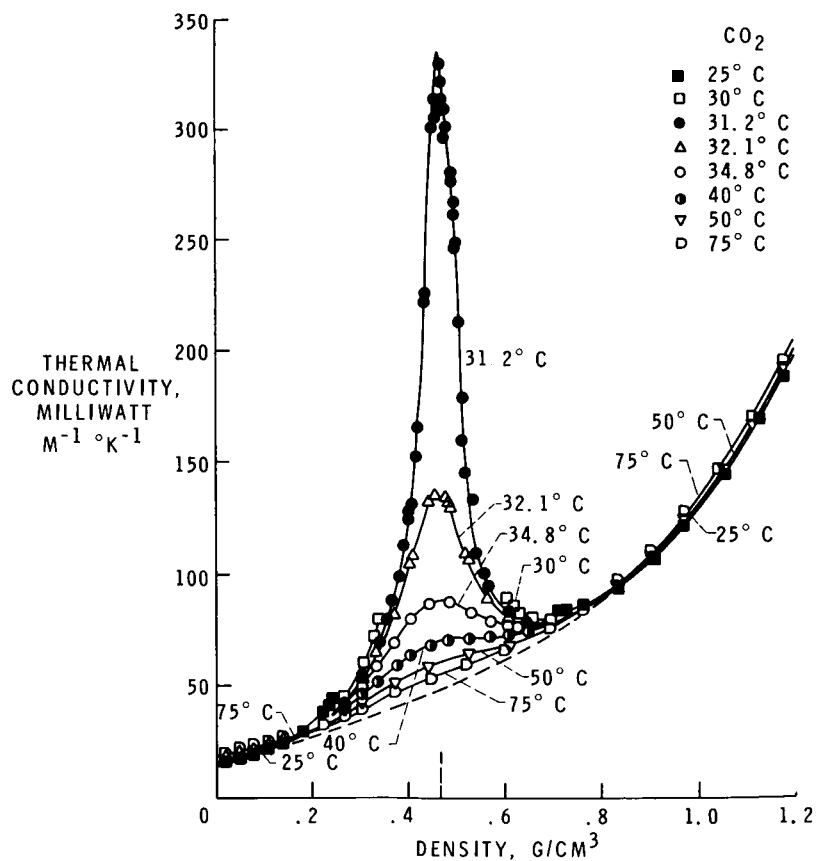


Figure 12. - The thermal conductivity of carbon dioxide (from Sengers (86)).



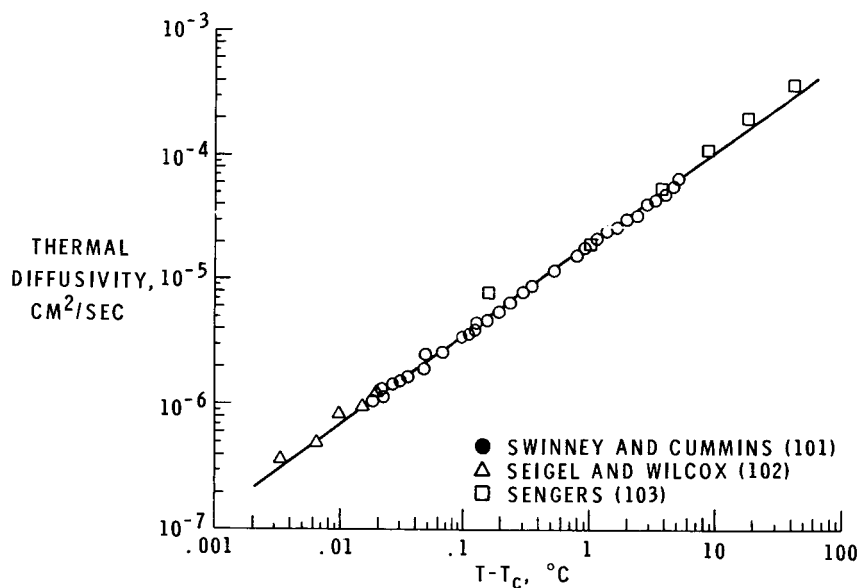


Figure 13. - Thermal diffusivity of carbon dioxide along the critical isochore (from Ref. 101).

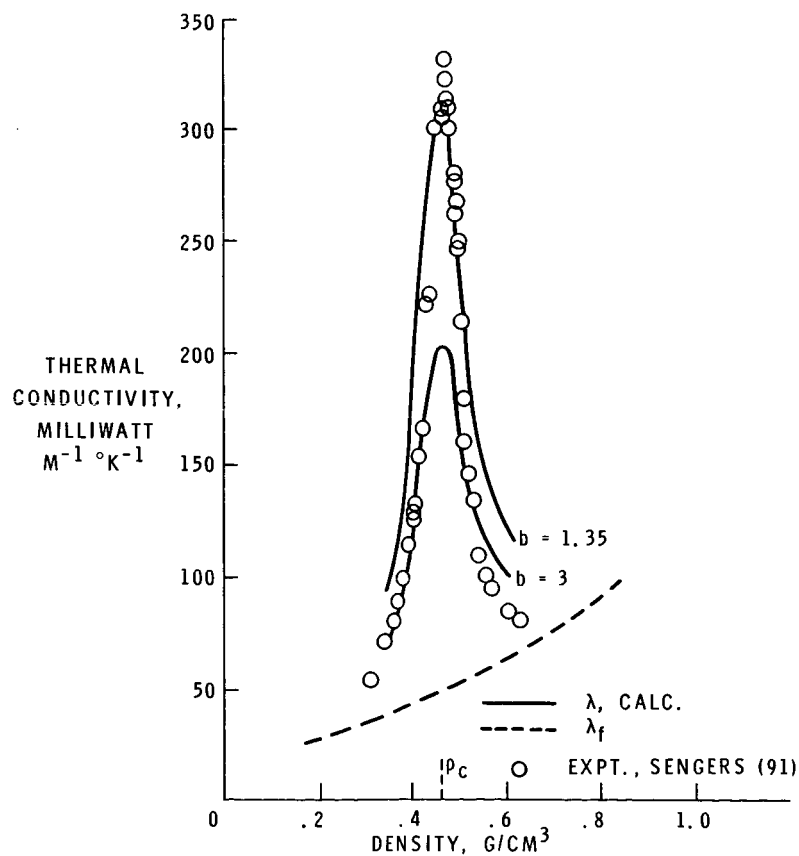


Figure 14. - Comparison of calculated and experimental thermal conductivities of carbon dioxide.  $T = 31.2^\circ\text{C}$  (Eqs. (37), (42), (45), and (48)).

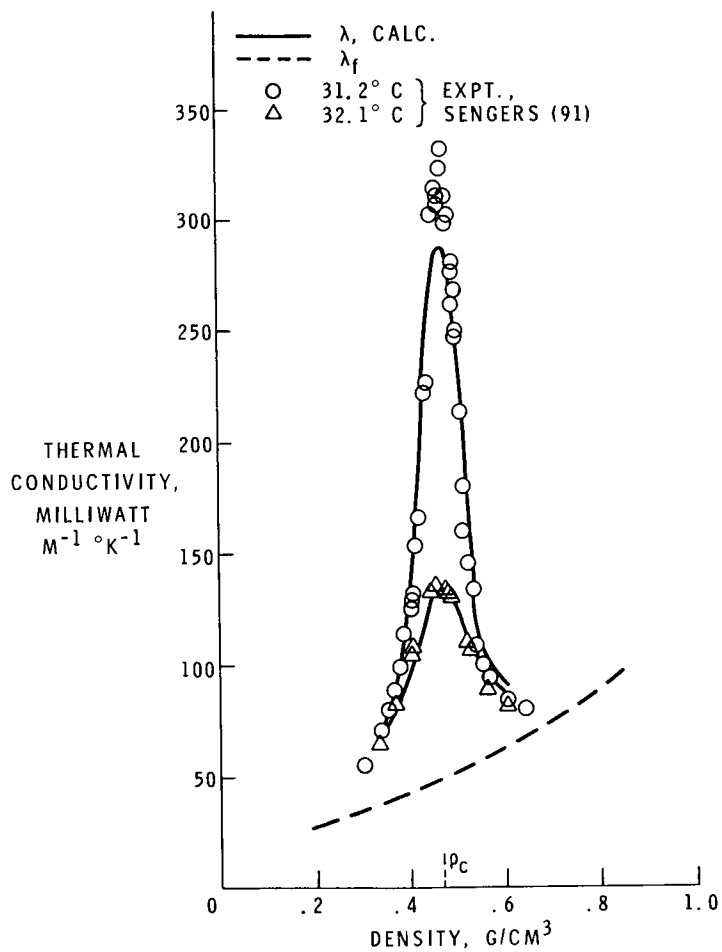


Figure 15. - Calculated and experimental thermal conductivities of carbon dioxide (Eqs. (37), (42), (48), and (49)).